Measurement of D-meson production and flow in Pb-Pb collisions with ALICE at the LHC

8th International Conference on New Frontiers in Physics, Kolymbari (Crete, Greece)

Fabio Catalano on behalf of the ALICE Collaboration

24 August 2019

Politecnico and INFN Torino, Italy

Quark-Gluon Plasma in ultra-relativistic heavy-ion collisions

Quantum chromodynamics (QCD) calculations predict a phase transition of nuclear matter to a colour-deconfined medium, the quark–gluon plasma (QGP), under extreme conditions of temperature and/or density

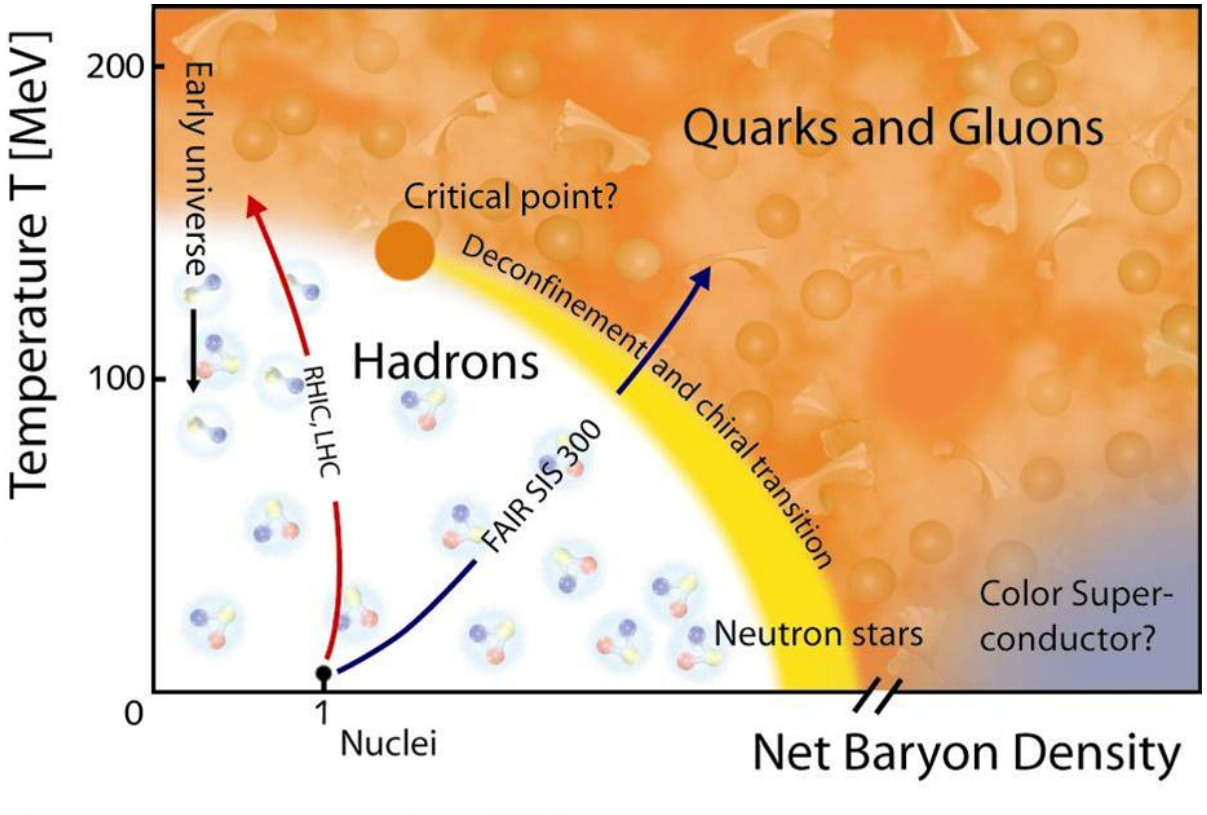

- The QGP can be created in the laboratory by ultra-relativistic heavy-ion collisions

Heavy flavours in Pb-Pb collisions

Large masses ($m_c \simeq 1.3\ \mathrm{GeV}/c^2$, $m_b \simeq 4.5\ \mathrm{GeV}/c^2$) of charm and beauty quarks
→ produced in hard-scattering processes in the early stages of the collision

- They experience the full evolution of the Quark-Gluon Plasma
- Negligible thermal production and annihilation in the medium
- Strongly interacting with the QGP

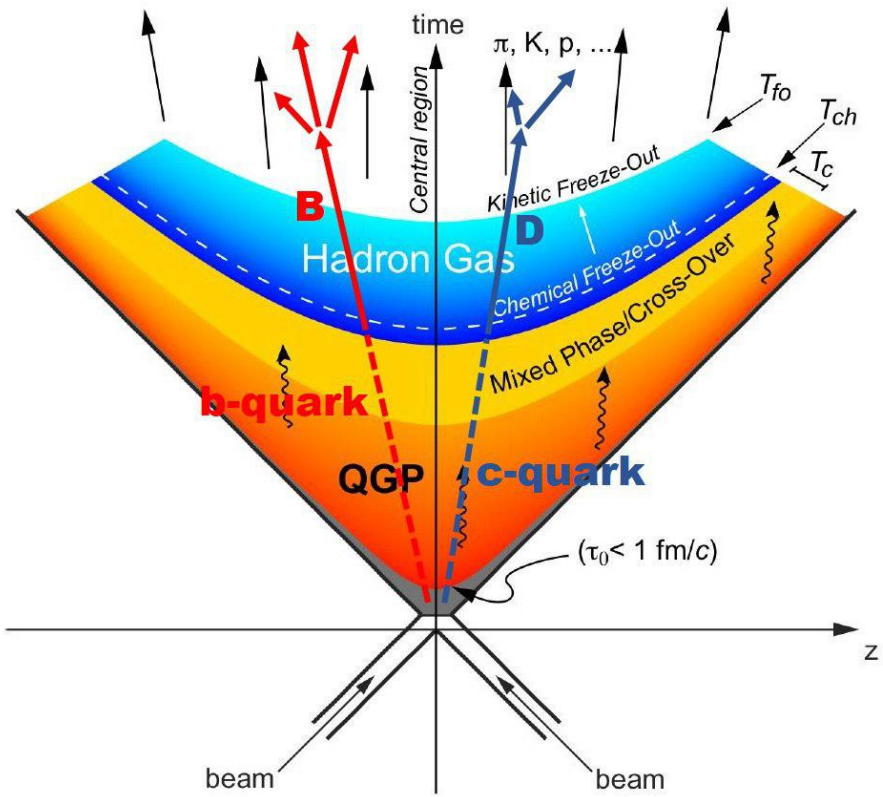

Heavy flavours are unique probes of the deconfined medium

Heavy flavours in Pb-Pb collisions — Observables

Heavy flavours propagate through the QGP and interact with the medium constituents

- **Energy loss via elastic scatterings and gluon radiation**, depending on
  - colour charge (Casimir factor)
  - quark mass (Dead-cone effect)
  - path length

$$\Delta E_g > \Delta E_{u,d,s} > \Delta E_c > \Delta E_b$$

Observable: Nuclear Modification Factor (R_{AA})

$$R_{\mathrm{AA}}\ (p_{\mathrm{T}}) = \frac{1}{\langle N_{coll}^{\mathrm{AA}} \rangle} \frac{dN_{\mathrm{AA}}/p_{\mathrm{T}}}{dN_{\mathrm{pp}}/p_{\mathrm{T}}}$$

Heavy flavours in Pb-Pb collisions — Observables

Heavy flavours propagate through the QGP and interact with the medium constituents

- Energy loss via elastic scatterings and gluon radiation
- **Participation in the collective motion of the fireball**
  - possible thermalisation of heavy quarks in the medium

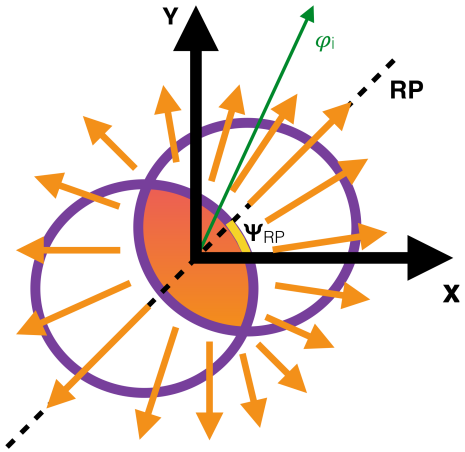

Observable: azimuthal anisotropy of produced particle momenta

Fourier decomposition of particle-momenta azimuthal distribution

$$E\frac{\mathrm{d}^3N}{\mathrm{d}p_\mathrm{T}} = \frac{1}{2\pi}\frac{\mathrm{d}^2N}{p_\mathrm{T}\mathrm{d}p_\mathrm{T}\mathrm{d}y}\left\{1+\sum_{n=1}^{\infty} v_n \cos[n(\varphi-\Psi_n)]\right\}$$

$$v_2 = \langle\cos[2(\varphi-\Psi_2)]\rangle$$

2nd harmonic coefficient

elliptic flow

Heavy flavours in Pb-Pb collisions — Observables

Heavy flavours propagate through the QGP and interact with the medium constituents

- Energy loss via elastic scatterings and gluon radiation
- Participation in the collective motion of the fireball
- **Modification of the hadronisation mechanism**
  - recombination with quarks from the medium

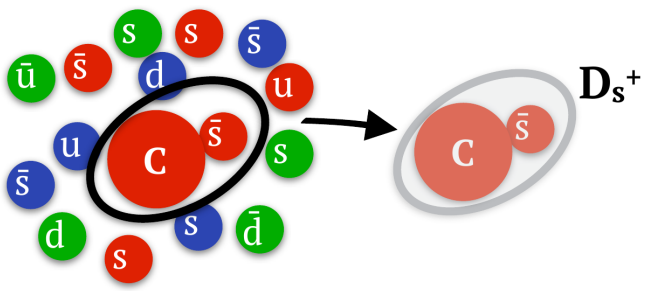

Observable: p_{T}-dependent yield ratios and R_{AA} of different hadron species

A Large Ion Collider Experiment

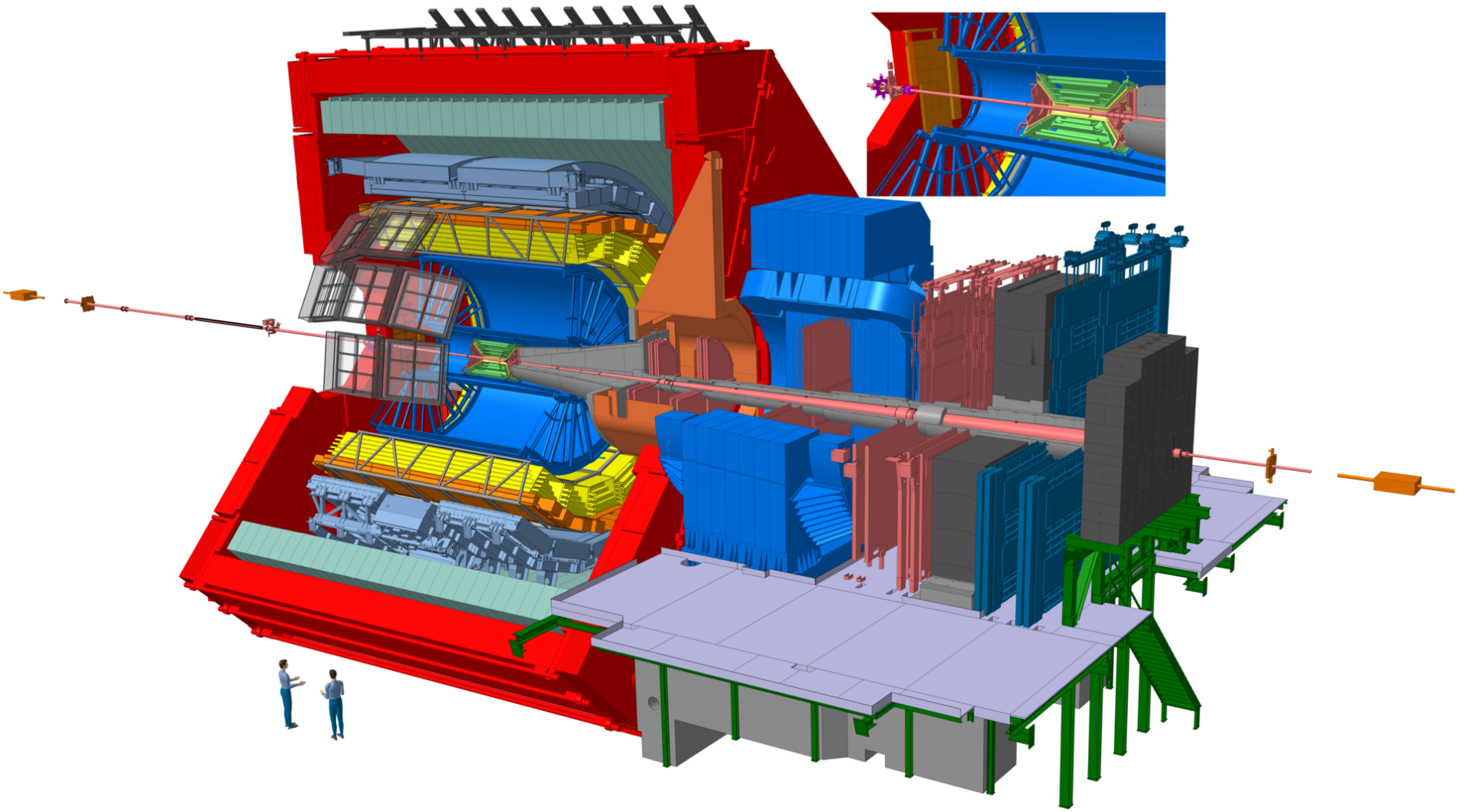

A Large Ion Collider Experiment

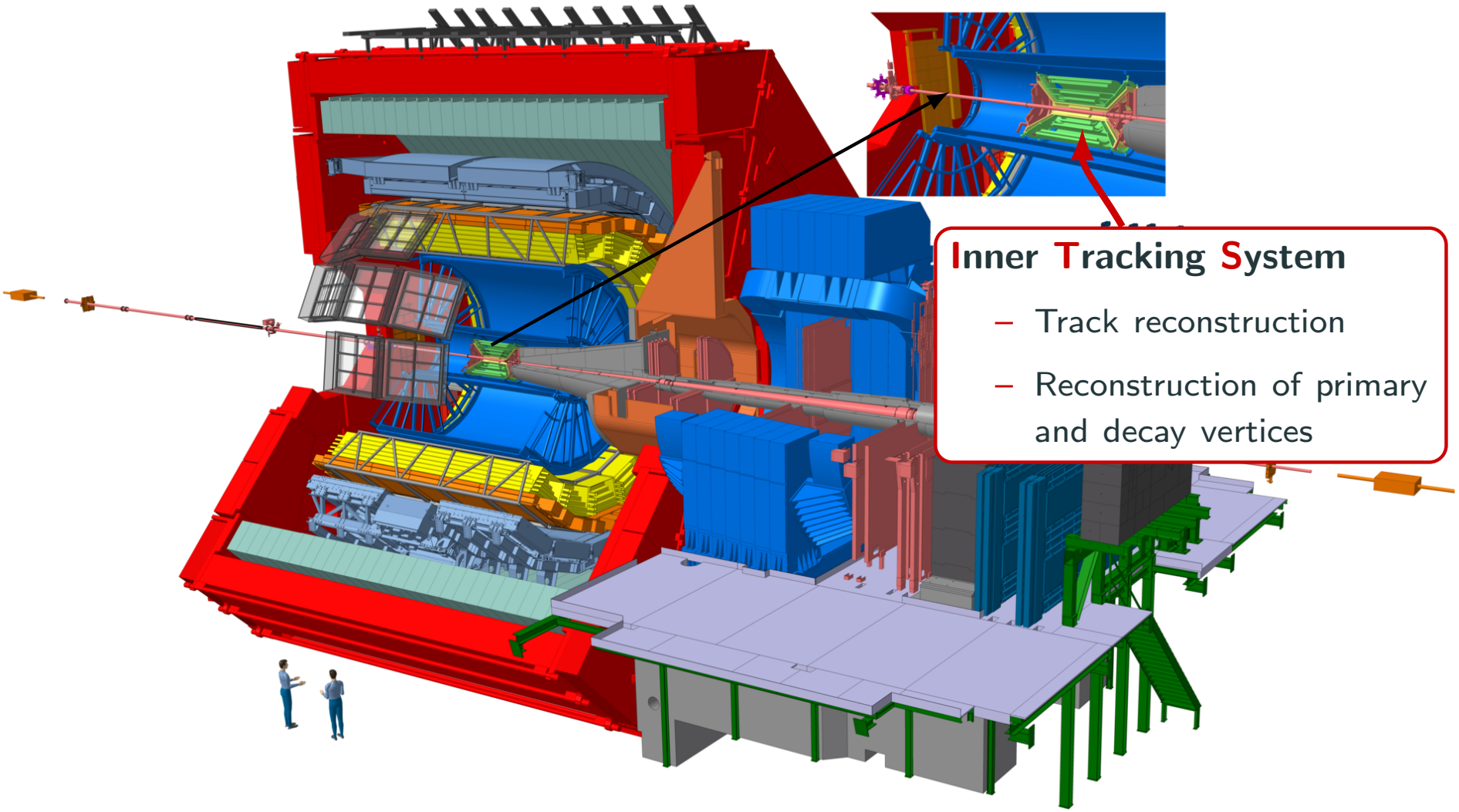

Inner Tracking System

- Track reconstruction
- Reconstruction of primary and decay vertices

A Large Ion Collider Experiment

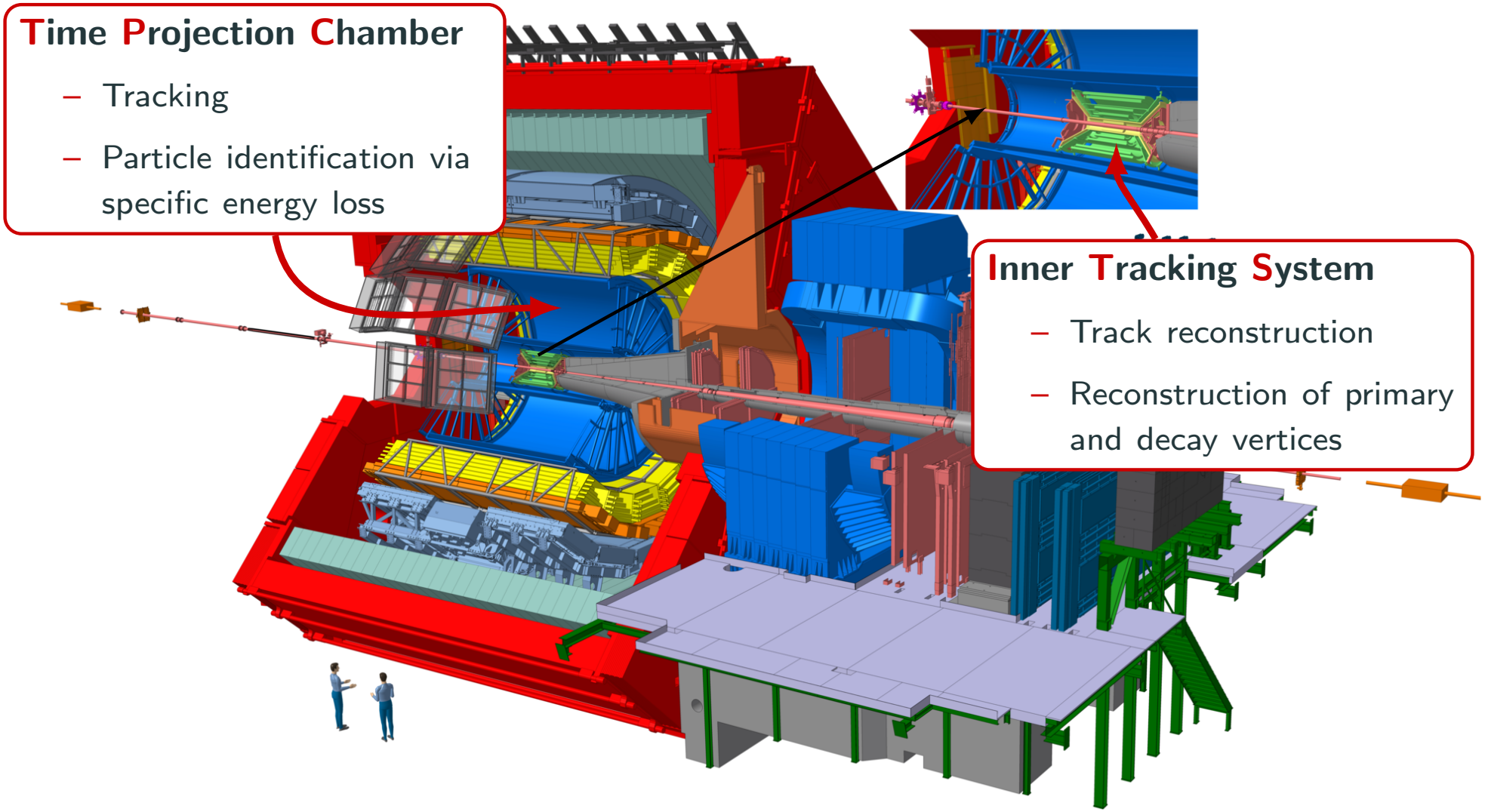

A Large Ion Collider Experiment

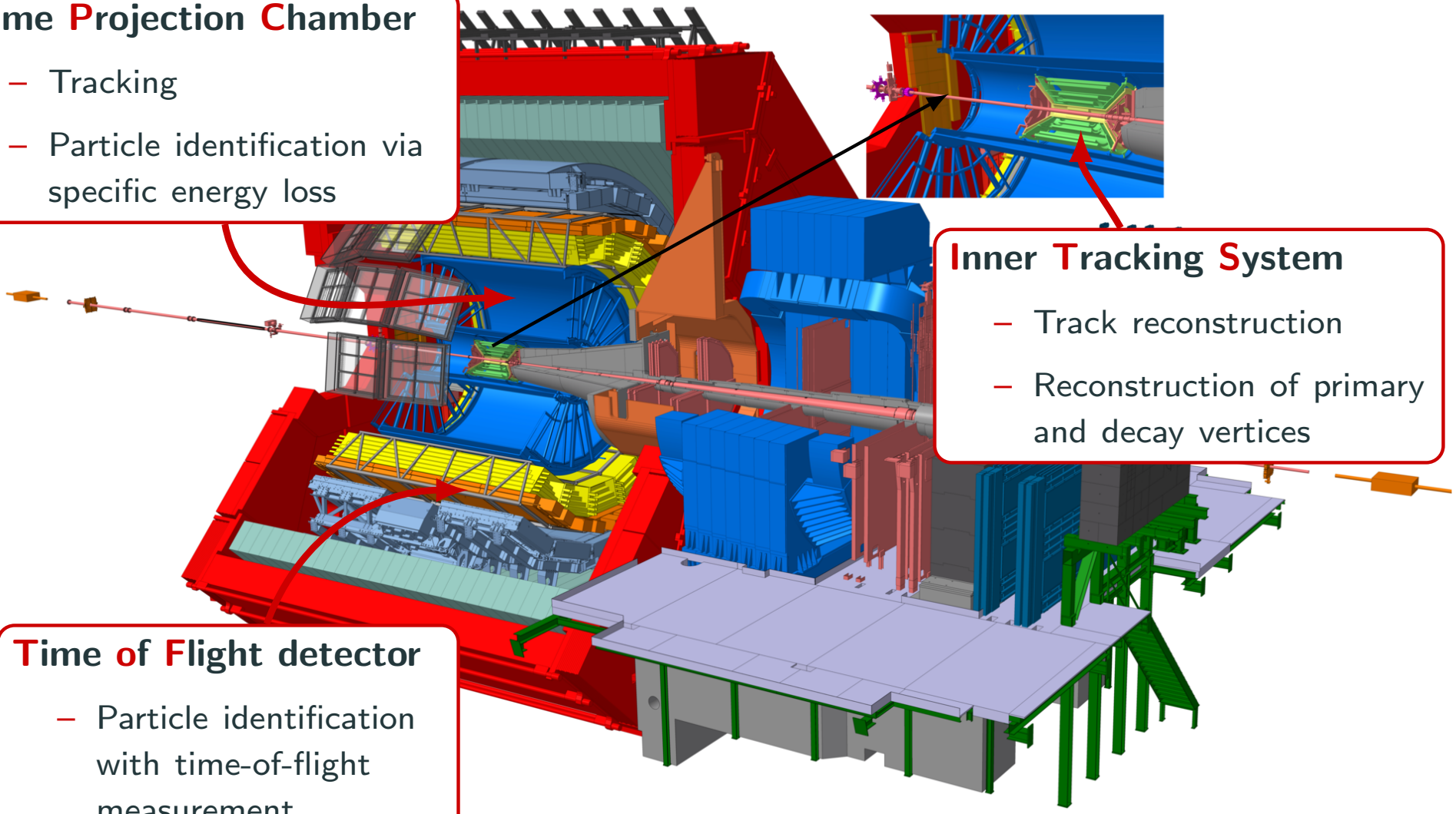

Time Projection Chamber

- Tracking
- Particle identification via specific energy loss

Inner Tracking System

- Track reconstruction
- Reconstruction of primary and decay vertices

Time of Flight detector

- Particle identification with time-of-flight measurement

A Large Ion Collider Experiment

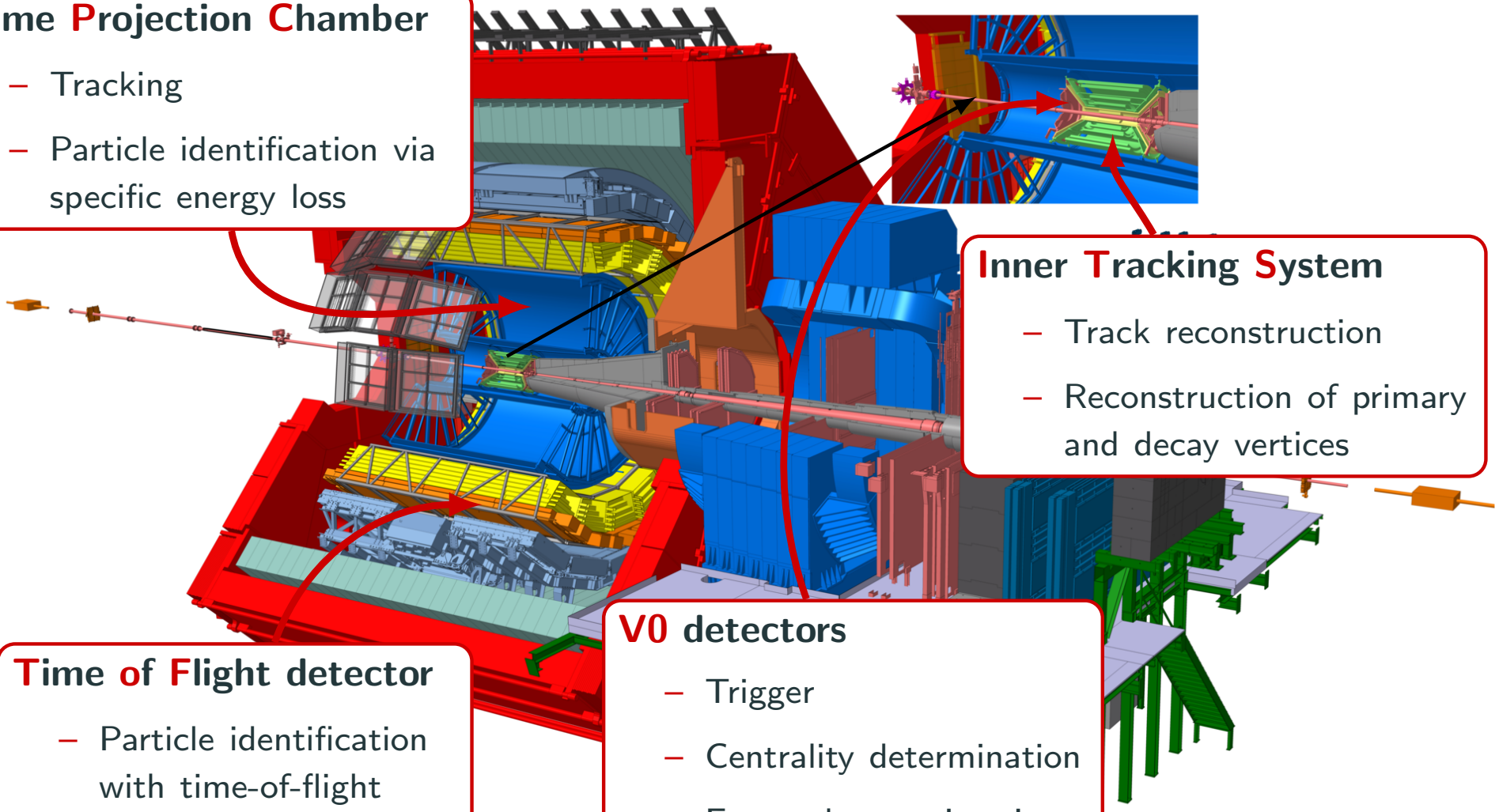

Time Projection Chamber

- Tracking
- Particle identification via specific energy loss

Inner Tracking System

- Track reconstruction
- Reconstruction of primary and decay vertices

Time of Flight detector

- Particle identification with time-of-flight measurement

V0 detectors

- Trigger
- Centrality determination
- Event-plane estimation

D-meson reconstruction

Meson	M (GeV/c^2)	Decay	$c\tau$ (μm)	BR (%)
D^0 ($c\bar{u}$)	~ 1.865	$K^-\pi^+$	~ 123	~ 3.89
D^+ ($c\bar{d}$)	~ 1.870	$K^-\pi^+\pi^+$	~ 312	~ 8.98
D^{*+} ($c\bar{d}$)	~ 2.010	$D^0(\to K^-\pi^+)\pi^+$	strong decay	~ 2.66
D_s^+ ($c\bar{s}$)	~ 1.968	$\phi(\to K^-K^+)\pi^+$	~ 151	~ 2.25

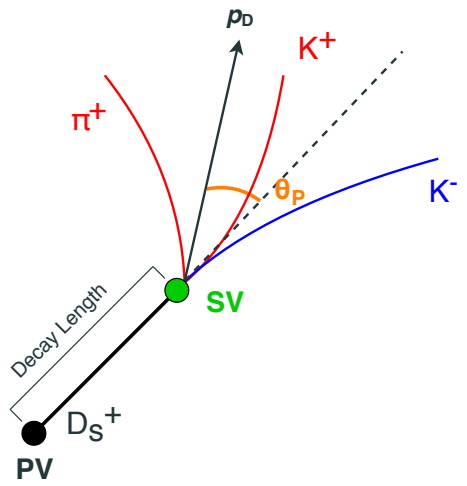

- Candidates built from pairs/triplets of tracks reconstructed at mid-rapidity ($|\eta| < 0.8$) with proper charge combination
- To reduce the background:
  - particle identification of decay tracks
  - geometrical and kinematical selections of displaced decay-vertex topology

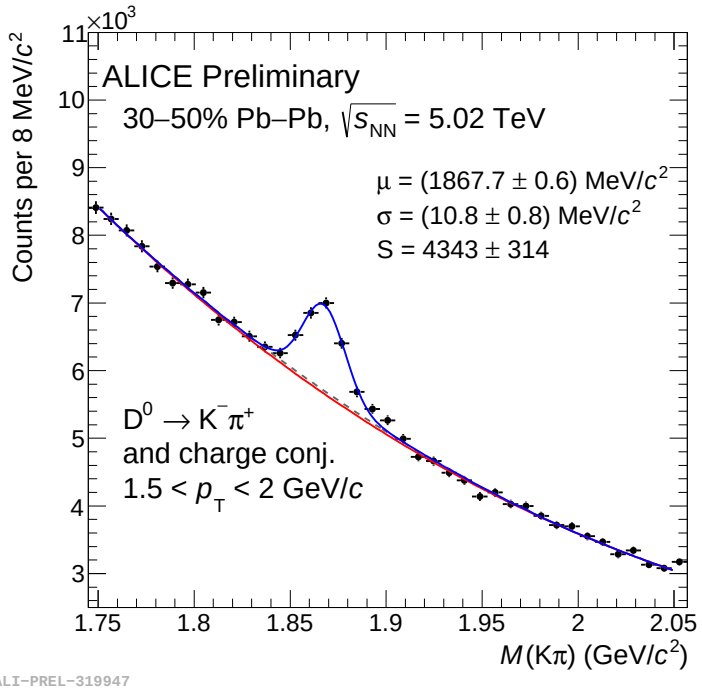

Non-strange D-meson R_{AA}

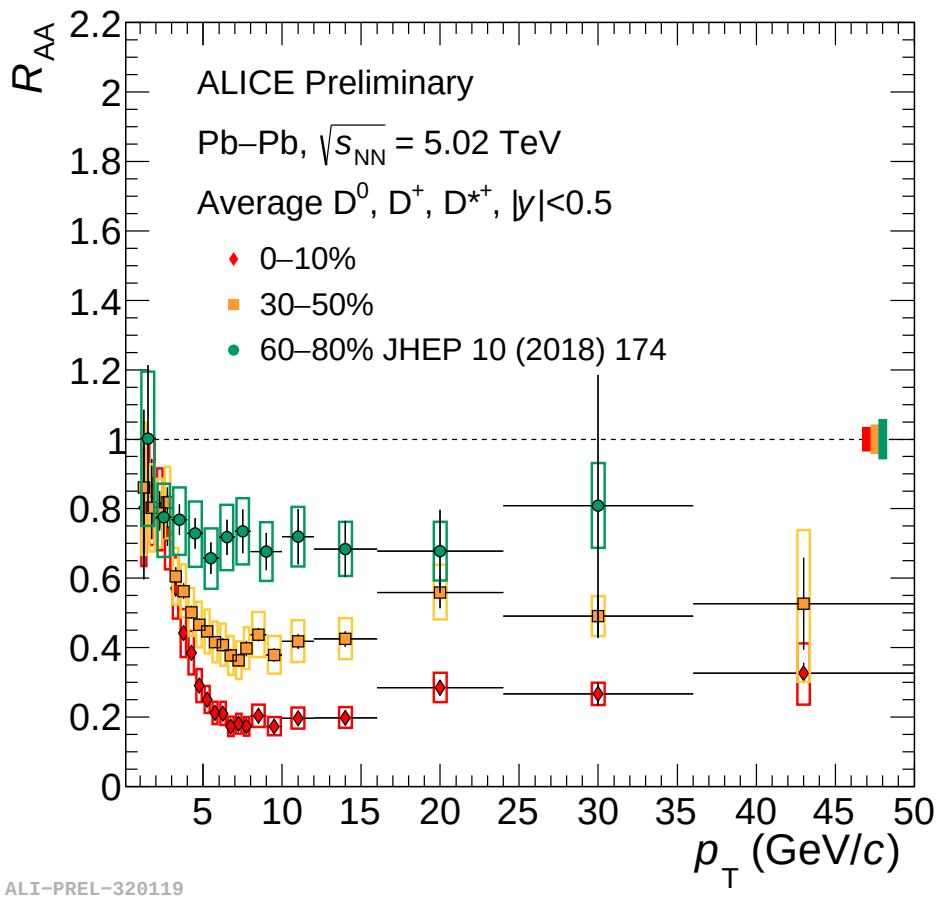

- D-meson $R_{AA} < 1$ observed → expected in presence of the QGP medium

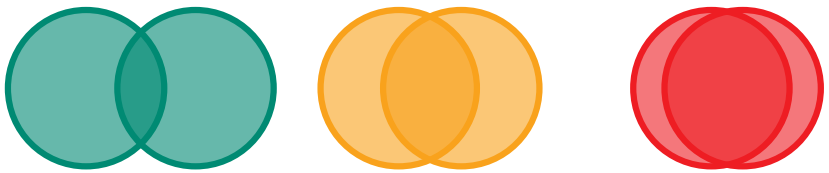

- Hierarchy in the suppression: increasing from peripheral to semi-central and central Pb-Pb collisions

- Strong suppression of R_{AA} in $0-10\%$ centrality class (factor ~ 5 in magnitude at $8-12$ GeV/c)

Non-strange D-meson R_{AA} — Flavour dependence

- $R_{AA}(\mathrm{D}) > R_{AA}(\pi^{\pm})$ for p_{T} below 8 GeV/c, many factors play a role:
  - pion production scaling with N_{part} at low p_{T}
  - different initial p_{T} shape and fragmentation functions
  - possible mass and color-charge effects
  - different effects of coalescence and radial flow on $\pi^{\pm}$ and D

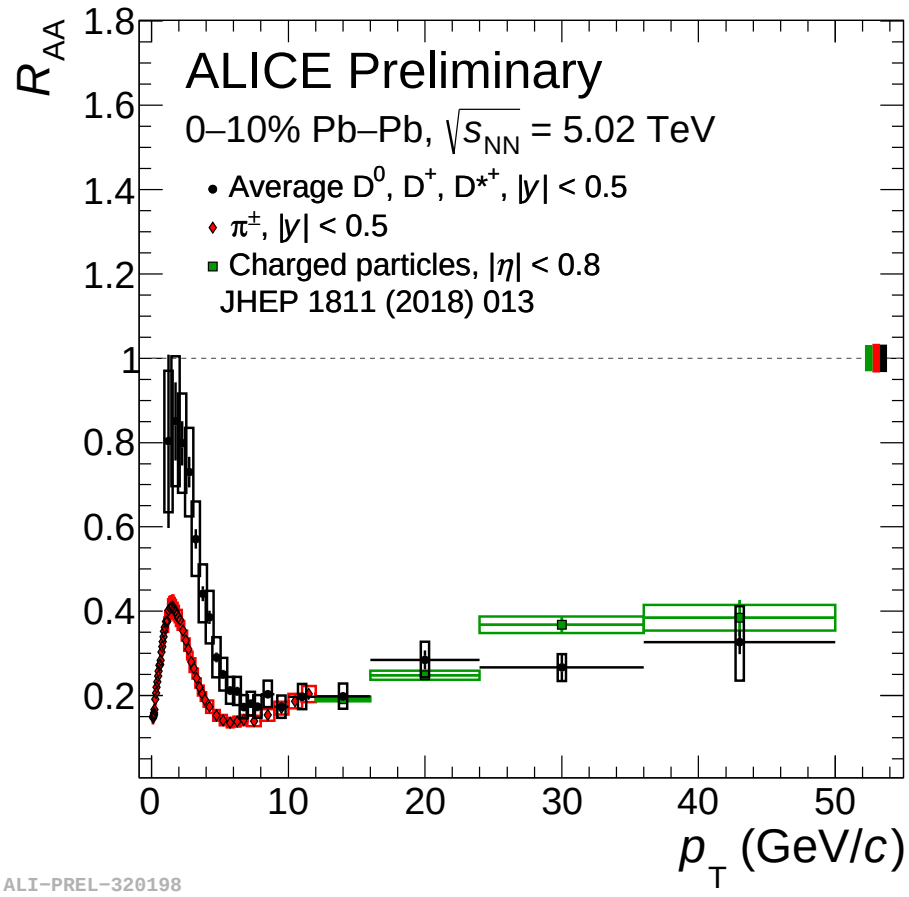

- $R_{AA}(\mathrm{D}) \simeq R_{AA}(\pi^{\pm}) \simeq R_{AA}$(*ch. part.*) for $p_{\mathrm{T}} > 8$ GeV/c
- Similar behaviour observed in semi-central collisions

Non-strange D-meson R_{AA} — Model comparison

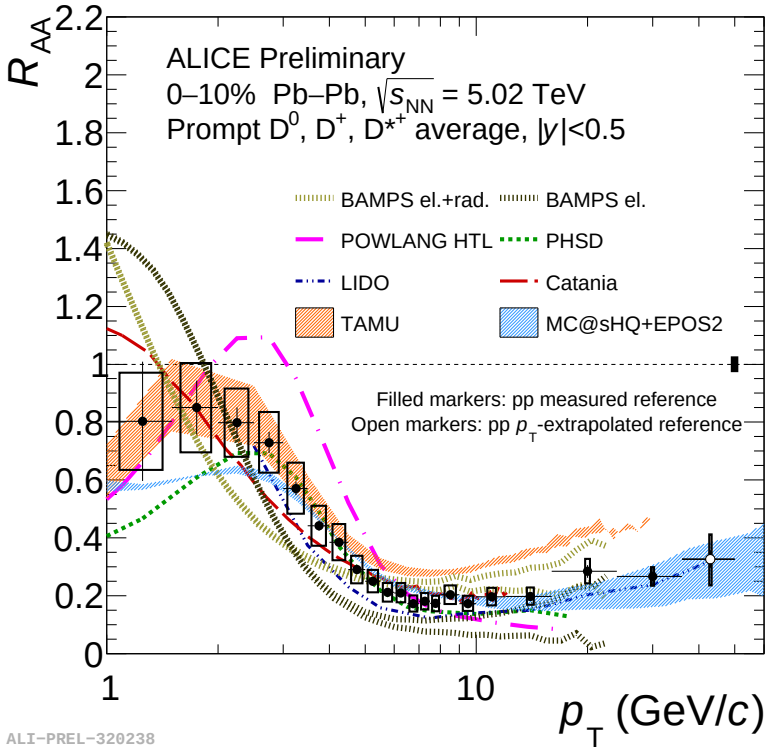

- Low p_{T} D-meson R_{AA} described by transport models
- TAMU, BAMPS el., POWLANG do not include radiative energy loss
  - data suggest that radiative energy loss is relevant at $p_{\mathrm{T}} > 6 - 8\ \mathrm{GeV}/c$
- BAMPS predictions, not including recombination, diverge from data at low p_{T}

BAMPS: JPG 42, 115106 (2015)
POWLANG: EPJC 75, 121 (2015)
LIDO: PRC 98, 064901 (2018)
TAMU: PLB 735, 445-450 (2014)

PHSD: PRC 92, 014910 (2015)
Catania: EPJC 78, 348 (2018)
MC@sHQ+EPOS: PRC 89, 014905 (2014)

Non-strange D-meson R_{AA} — Model comparison

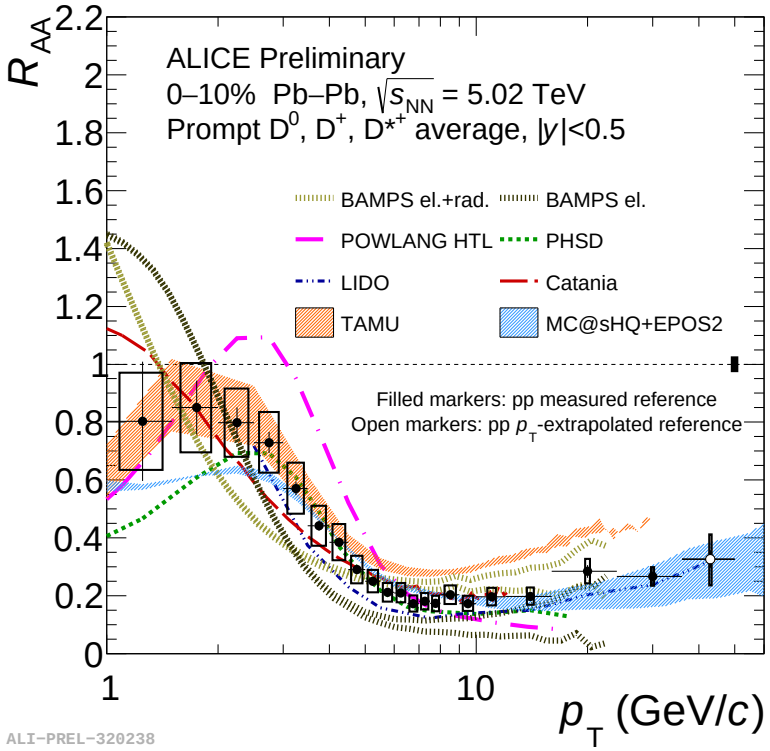

- Low p_T D-meson R_{AA} described by transport models

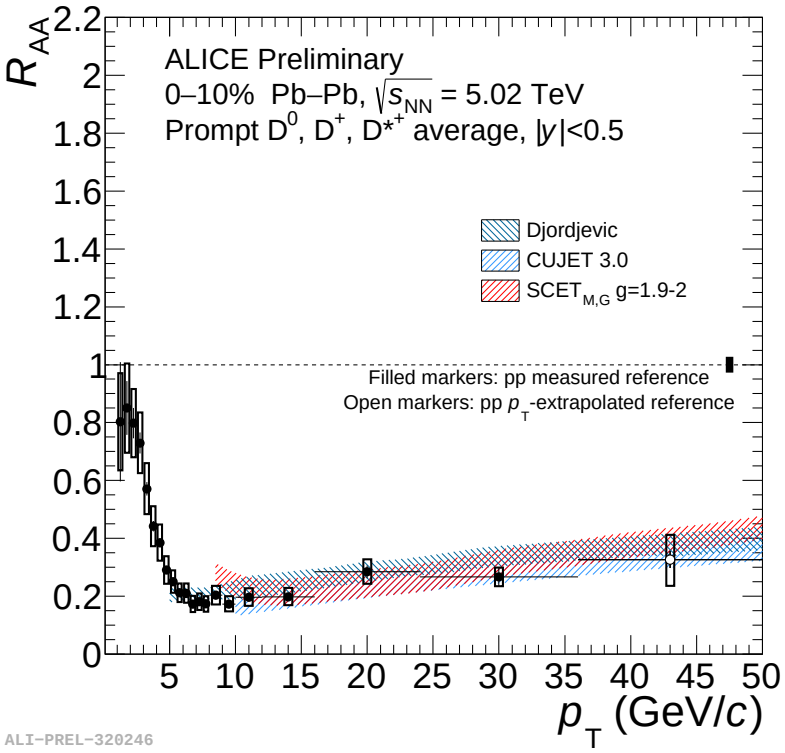

- High p_T D-meson R_{AA} described by pQCD-based energy-loss models

Djordjevic: PRC 92, 024918 (2015)
CUJET3.0: JHEP 02 (2016) 169
SCET: JHEP 03 (2017) 146

Strange and non-strange D-meson R_{AA}

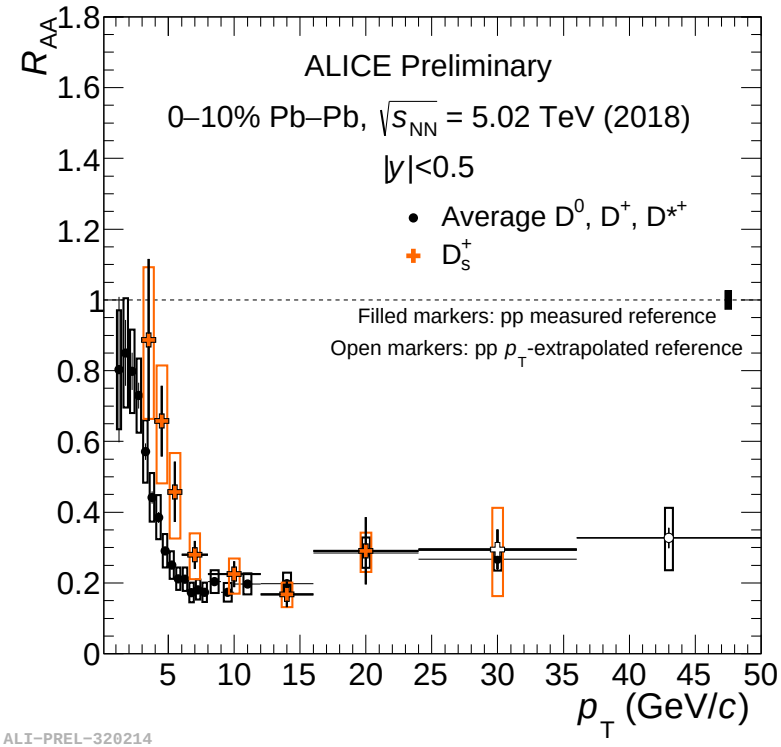

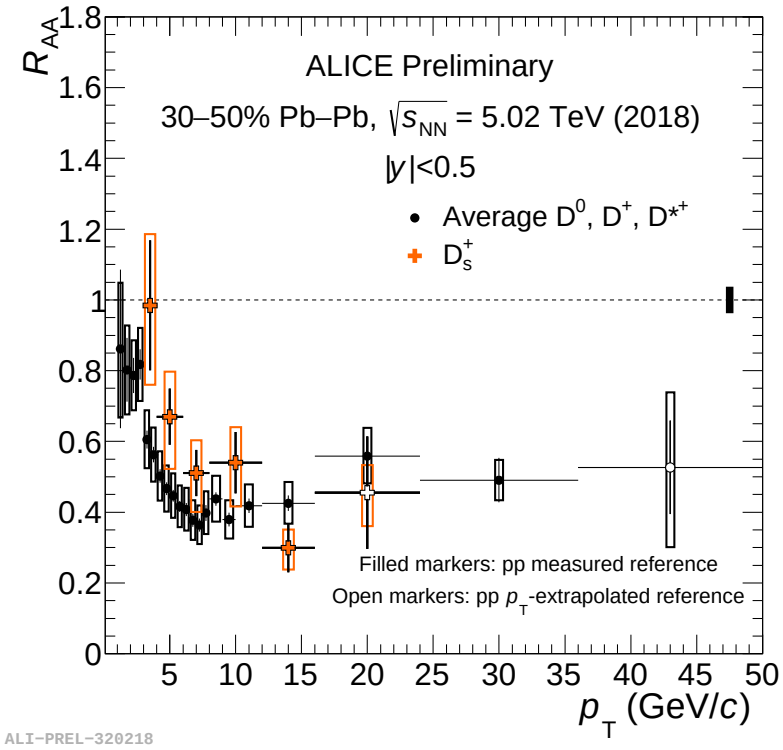

- $\mathrm{D_s^+}$ and non-strange D-meson R_{AA} show a similar p_{T} dependence
- Hint of smaller suppression of $\mathrm{D_s^+}$ mesons w.r.t. non-strange D mesons at $p_{\mathrm{T}} < 8\ \mathrm{GeV}/c$, both in $0-10\%$ and $30-50\%$
  - as expected in case of hadronization via coalescence + strangeness enhancement in the QGP, EPJ C51 (2007) 113

Strange and non-strange D-meson R_{AA}

PHSD: PRC 92, 014910 (2015) TAMU: PLB 735, 445-450 (2014) Catania: EPJC 78, 348 (2018)

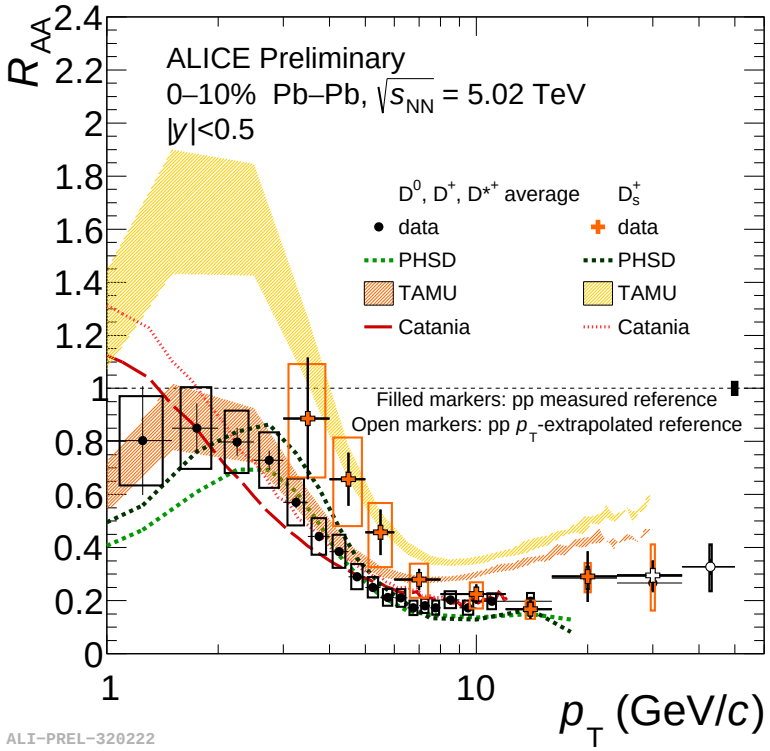

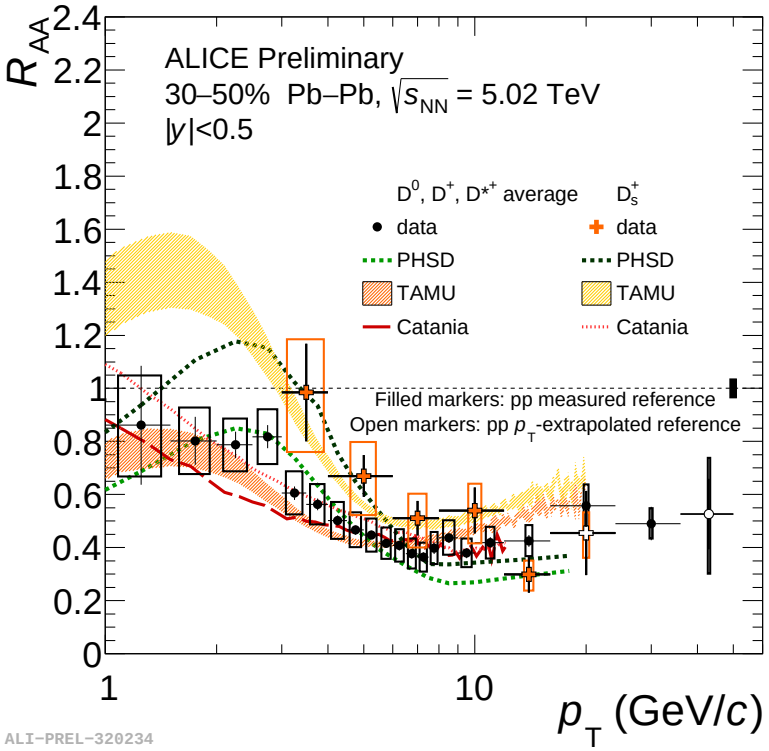

- D_s^+ and non-strange D-meson R_{AA} show a similar p_T dependence
- Hint of smaller suppression of D_s^+ mesons w.r.t. non-strange D mesons at $p_T < 8$ GeV/c, both in $0-10\%$ and $30-50\%$
- Models including coalescence describe the hierarchy $R_{AA}(D_s^+) > R_{AA}(D)$

Non-strange D-meson abundances in Pb-Pb collisions

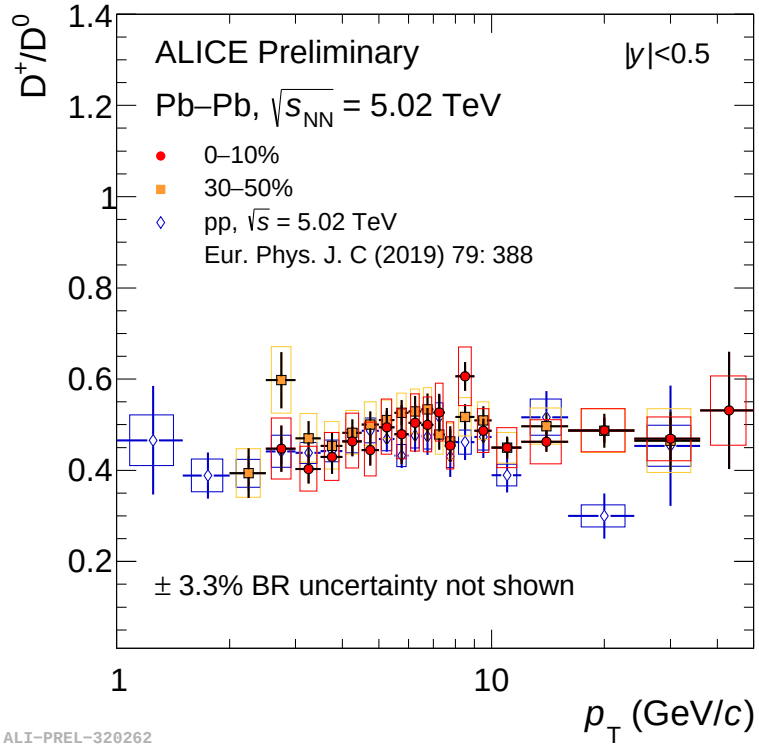

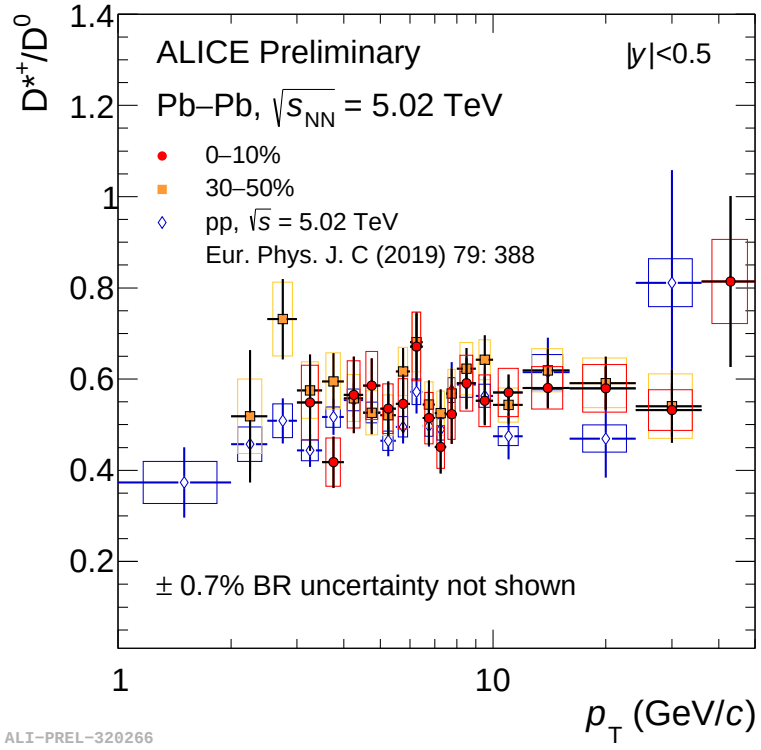

- Non-strange D-meson relative abundances → no modification is observed from pp to Pb-Pb collisions
- Compatible ratios between $0-10\%$ and $30-50\%$ centrality classes

D_s meson abundance in Pb-Pb collisions

TAMU: PLB 735, 445-450 (2014) Catania: EPJC 78, 348 (2018) PHSD: PRC 92, 014910 (2015)

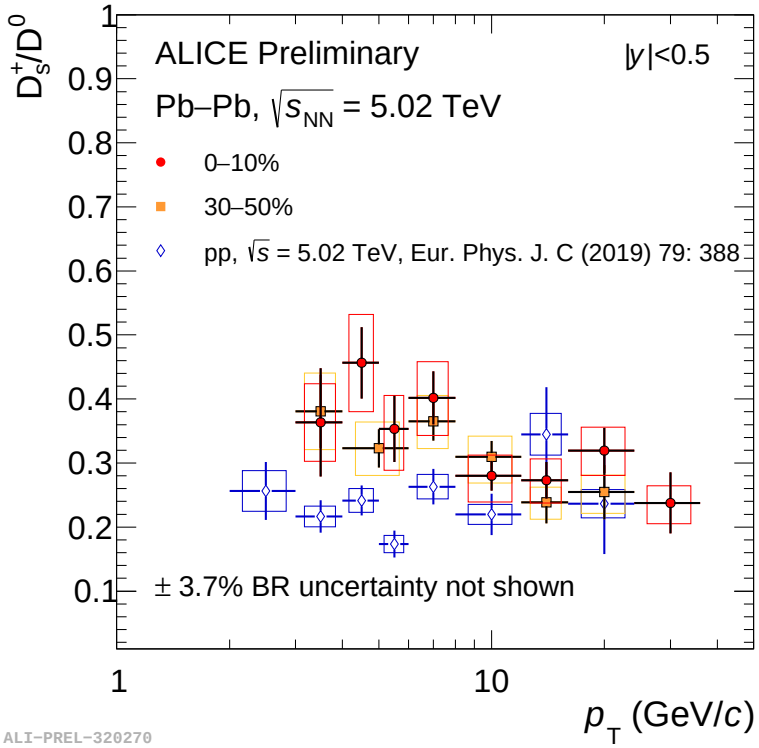

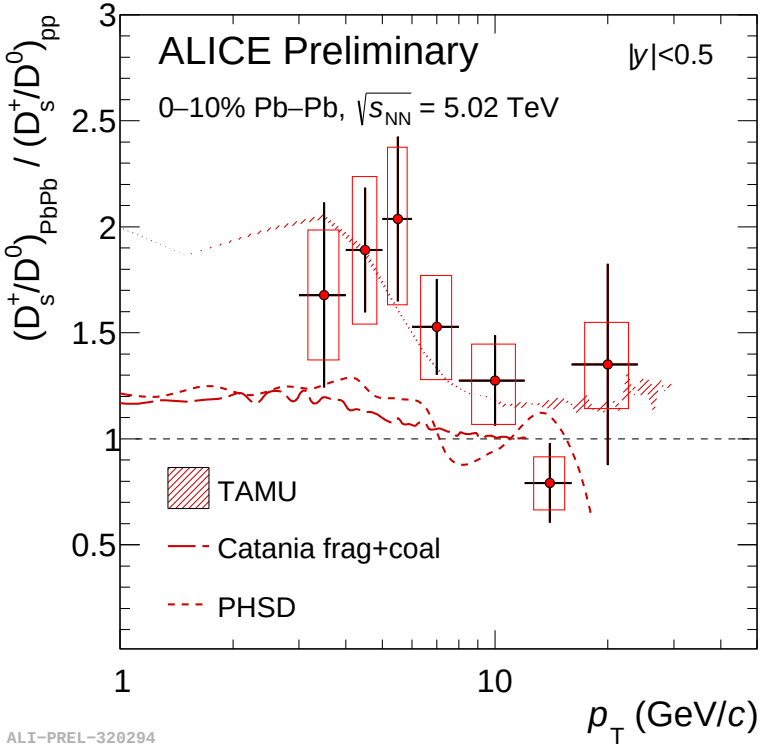

- Indication of an higher D_s^+/D^0 ratio in Pb-Pb collisions than in pp at $p_T < 8$ GeV/c, both for central and semi-central collisions
- p_T-trend of double ratio qualitatively described by transport models including hadronisation via recombination

Non-strange D-meson elliptic flow in Pb-Pb collisions

Positive D-meson v_2 in semi-central Pb-Pb collisions → participation of charm quark in the collective motion of the system

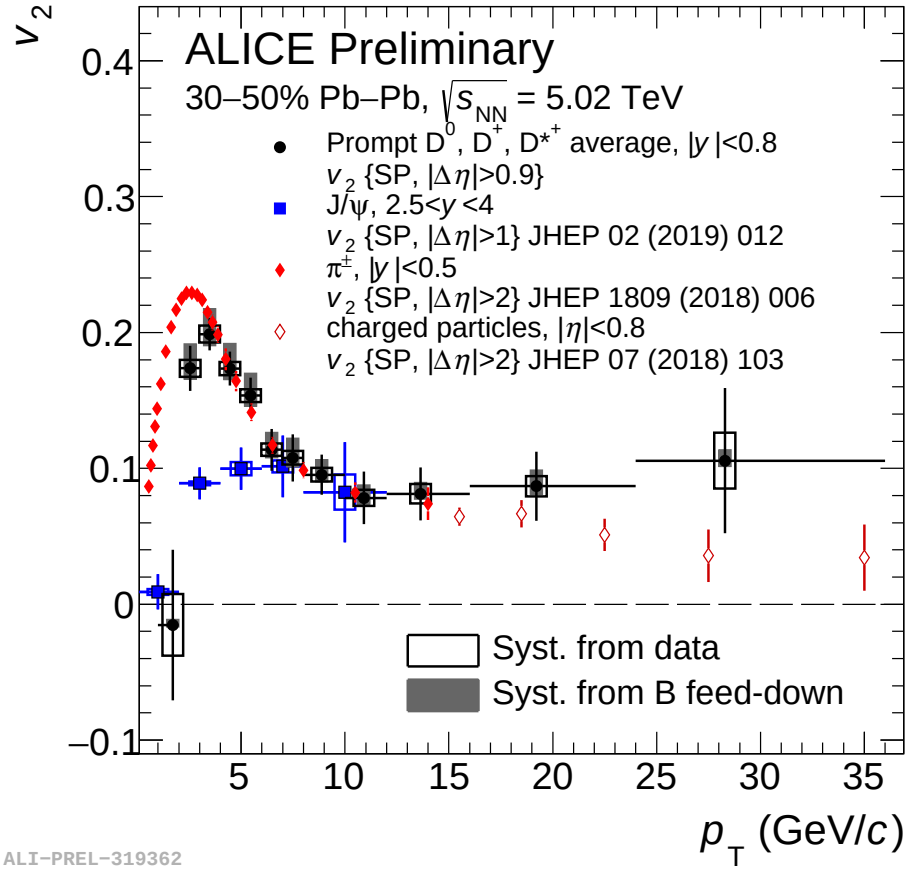

- Hint of $v_2(\mathrm{D}) < v_2(\pi^{\pm})$ for $p_{\mathrm{T}} < 4\ \mathrm{GeV}/c$
- $v_2(\mathrm{D}) \simeq v_2(\pi^{\pm}) \simeq v_2(\textit{ch. part.})$ for $p_{\mathrm{T}} > 4\ \mathrm{GeV}/c$
- $v_2(\mathrm{D}) > v_2(J/\Psi)$ for $p_{\mathrm{T}} < 6\ \mathrm{GeV}/c$
  - coalescence of charm quarks with flowing light-flavour quarks

Non-strange D-meson elliptic flow — Model comparison

- Non-strange D-meson v_2 reproduced by theoretical models based on charm-quark transport
- Simultaneous prediction of D-meson R_{AA} and v_2:
  - important constraints on models
  - estimation of QGP transport coefficients

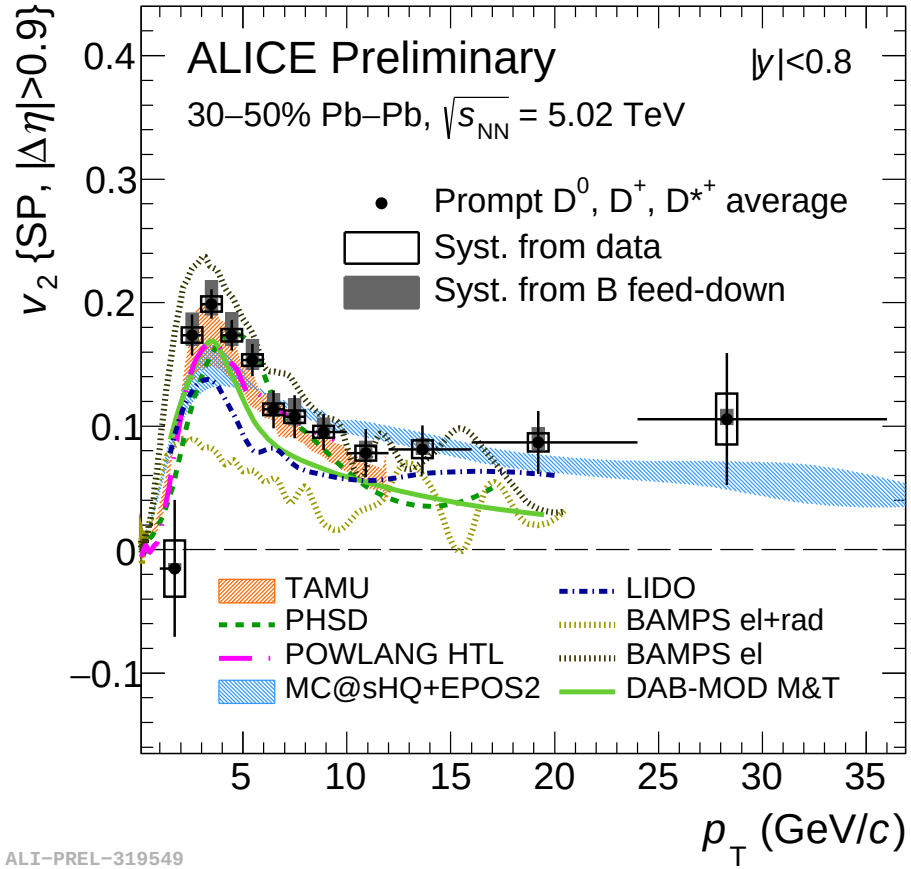

TAMU: arXiv:1905.09216
PHSD: PRC 92, 014910 (2015)
POWLANG: EPJC 75, 121 (2015)

MC@sHQ+EPOS: PRC 89, 014905 (2014)
LIDO: PRC 98, 064901 (2018)

BAMPS: JPG 42, 115106 (2015)
DAB-MOD: PRC 96, 064903 (2016)

Strange and non-strange D-meson elliptic flow

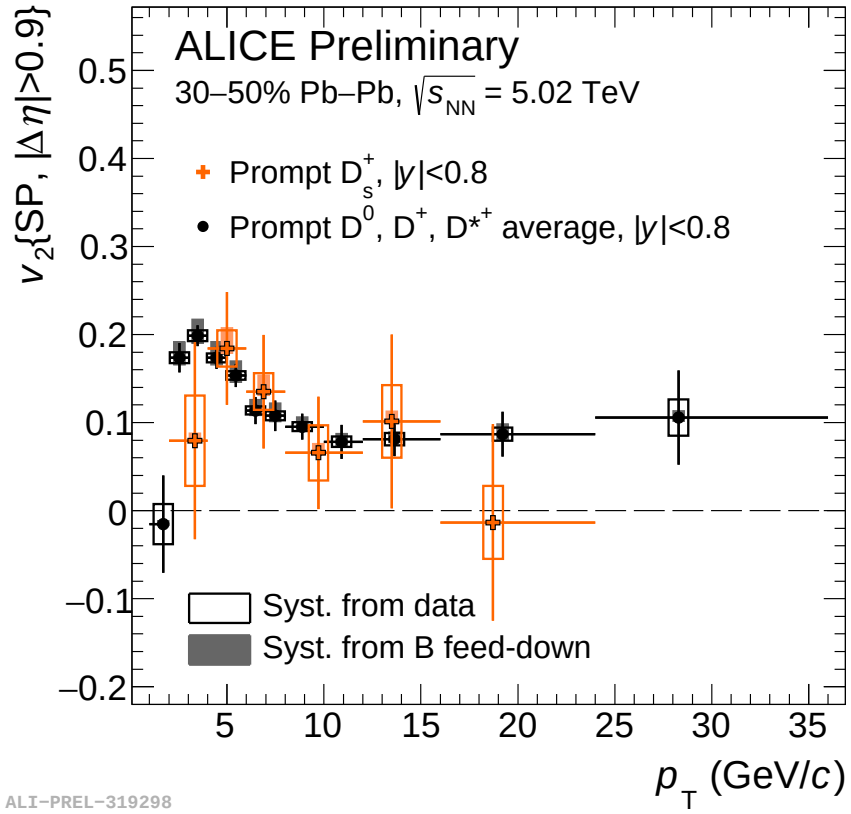

- Similar elliptic flow for strange and non-strange D mesons, within the large uncertainties

Strange and non-strange D-meson elliptic flow

TAMU: arXiv:1905.09216 PHSD: PRC 92, 014910 (2015)

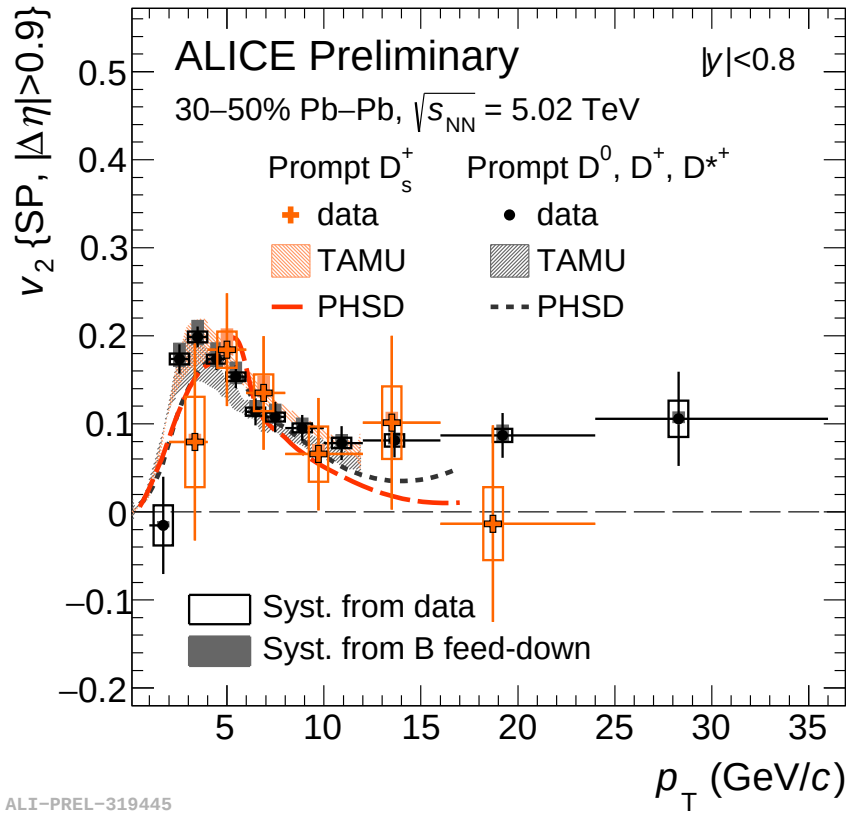

- Similar elliptic flow for strange and non-strange D mesons, within the large uncertainties
- v_2 of D_s^+ and non-strange D mesons predicted to be similar by models (TAMU and PHSD) ➔ including hadronisation via quark recombination

Event-shape engineering for D-meson v_2

- Event-shape engineering (ESE) ➔ event classification according to their eccentricity
- Magnitude of the second-harmonic reduced flow vector* used

$$q_2 = |\vec{Q}_2|/\sqrt{M}$$

20% smallest q_2 — $\langle v_2 \rangle_{small-q_2} < \langle v_2 \rangle_{unb.}$

20% largest q_2 — $\langle v_2 \rangle_{large-q_2} > \langle v_2 \rangle_{unb.}$

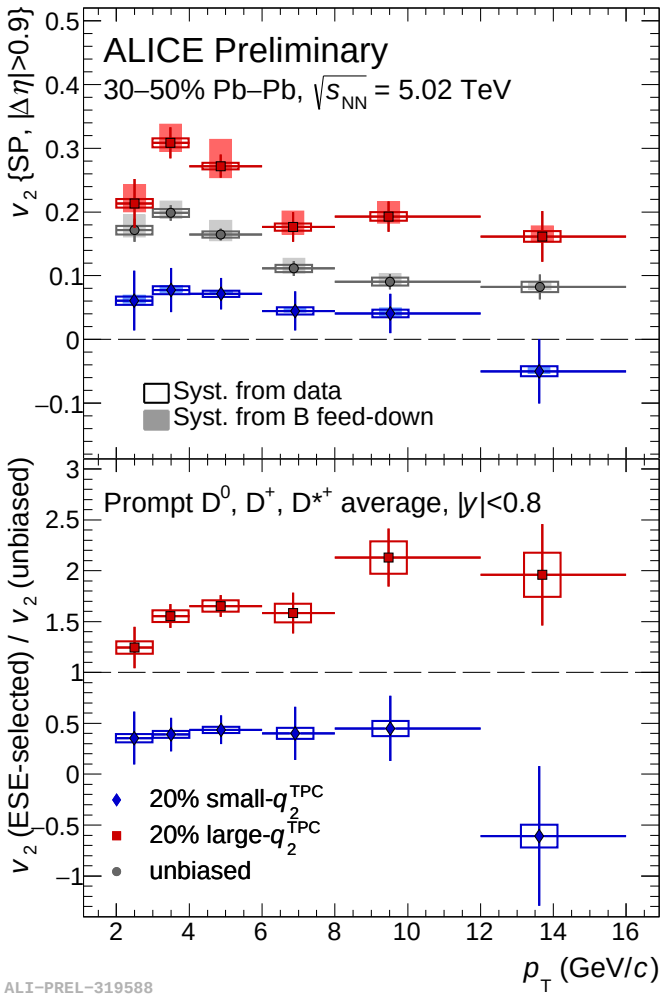

- Measurement of D-meson v_2 in ESE-selected samples ➔ charm sensitive to collectivity of light-hadron bulk and event-by-event fluctuations

*more details in the backup

ESE for D-meson v_2 — Model comparison

POWLANG: EPJC (2019) 79: 494 LIDO: PRC 98, 064901 (2018) DAB-MOD: PRC 96, 064903 (2016)

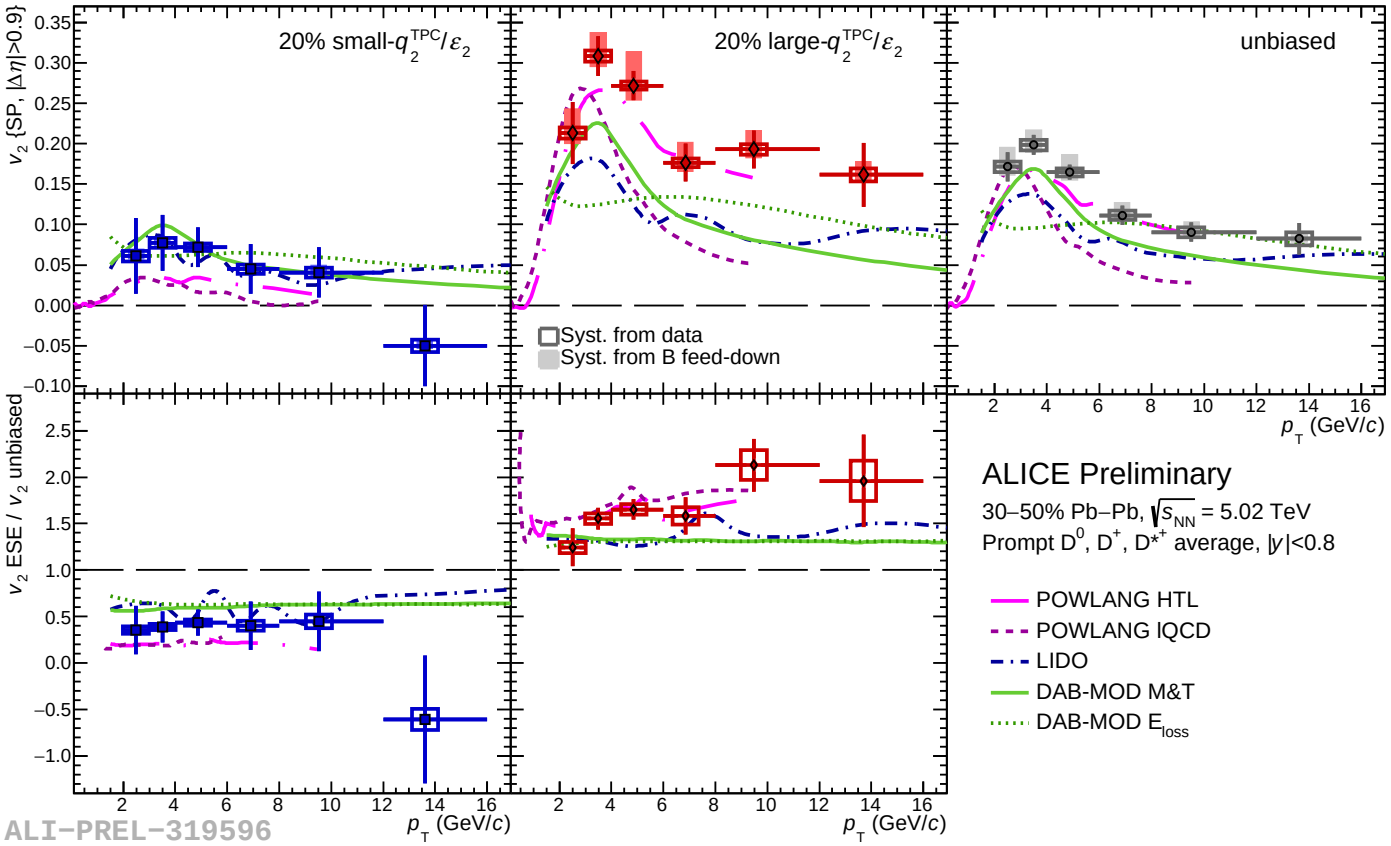

- Models based on charm-quark transport in an hydrodynamically expanding medium → describe q_2 dependence of elliptic flow
- Variation of D-meson v_2 in ESE-selected samples w.r.t. unbiased sample similar for different transport parameters (e.g. POWLANG HLT vs. lQCD)

Conclusion

- Suppression of non-strange D-meson R_{AA} in Pb-Pb collisions at $\sqrt{s_{\mathrm{NN}}} = 5.02$ TeV → charm-quark energy loss in the QGP
- $R_{\mathrm{AA}}(\mathrm{D}) > R_{\mathrm{AA}}(\textit{light hadron})$ at $p_{\mathrm{T}} < 8\ \mathrm{GeV}/c$ observed
- Indication of $R_{\mathrm{AA}}(\mathrm{D_s^+}) > R_{\mathrm{AA}}(D)$ and increase of the $\mathrm{D_s^+}/\mathrm{D^0}$ ratio in central and semi-central collisions
- Positive D-meson elliptic flow and similar v_2 between strange and non-strange D mesons → participation of charm quark in the medium collective motions
- Correlation between D mesons and light-hadron v_2 measured with ESE technique

Conclusion

- Suppression of non-strange D-meson R_{AA} in Pb-Pb collisions at $\sqrt{s_{\mathrm{NN}}} = 5.02$ TeV → charm-quark energy loss in the QGP
- $R_{\mathrm{AA}}(\mathrm{D}) > R_{\mathrm{AA}}(\textit{light hadron})$ at $p_{\mathrm{T}} < 8\ \mathrm{GeV}/c$ observed
- Indication of $R_{\mathrm{AA}}(\mathrm{D_s^+}) > R_{\mathrm{AA}}(D)$ and increase of the $\mathrm{D_s^+}/\mathrm{D^0}$ ratio in central and semi-central collisions
- Positive D-meson elliptic flow and similar v_2 between strange and non-strange D mesons → participation of charm quark in the medium collective motions
- Correlation between D mesons and light-hadron v_2 measured with ESE technique

Conclusion

- Suppression of non-strange D-meson R_{AA} in Pb-Pb collisions at $\sqrt{s_{\mathrm{NN}}} = 5.02$ TeV → charm-quark energy loss in the QGP
- $R_{\mathrm{AA}}(\mathrm{D}) > R_{\mathrm{AA}}(\textit{light hadron})$ at $p_{\mathrm{T}} < 8\ \mathrm{GeV}/c$ observed
- Indication of $R_{\mathrm{AA}}(\mathrm{D_s^+}) > R_{\mathrm{AA}}(D)$ and increase of the $\mathrm{D_s^+}/\mathrm{D^0}$ ratio in central and semi-central collisions
- Positive D-meson elliptic flow and similar v_2 between strange and non-strange D mesons → participation of charm quark in the medium collective motions
- Correlation between D mesons and light-hadron v_2 measured with ESE technique

Conclusion

- Suppression of non-strange D-meson R_{AA} in Pb-Pb collisions at $\sqrt{s_{\mathrm{NN}}} = 5.02$ TeV → charm-quark energy loss in the QGP
- $R_{\mathrm{AA}}(\mathrm{D}) > R_{\mathrm{AA}}(\textit{light hadron})$ at $p_{\mathrm{T}} < 8\ \mathrm{GeV}/c$ observed
- Indication of $R_{\mathrm{AA}}(\mathrm{D_s^+}) > R_{\mathrm{AA}}(D)$ and increase of the $\mathrm{D_s^+}/\mathrm{D^0}$ ratio in central and semi-central collisions
- Positive D-meson elliptic flow and similar v_2 between strange and non-strange D mesons → participation of charm quark in the medium collective motions
- Correlation between D mesons and light-hadron v_2 measured with ESE technique

Conclusion

- Suppression of non-strange D-meson R_{AA} in Pb-Pb collisions at $\sqrt{s_{\mathrm{NN}}} = 5.02$ TeV → charm-quark energy loss in the QGP
- $R_{\mathrm{AA}}(\mathrm{D}) > R_{\mathrm{AA}}(\textit{light hadron})$ at $p_{\mathrm{T}} < 8\ \mathrm{GeV}/c$ observed
- Indication of $R_{\mathrm{AA}}(\mathrm{D_s^+}) > R_{\mathrm{AA}}(D)$ and increase of the $\mathrm{D_s^+}/\mathrm{D^0}$ ratio in central and semi-central collisions
- Positive D-meson elliptic flow and similar v_2 between strange and non-strange D mesons → participation of charm quark in the medium collective motions
- Correlation between D mesons and light-hadron v_2 measured with ESE technique

Backup

Non-strange D-meson R_{AA} — Comparison with 2015 data

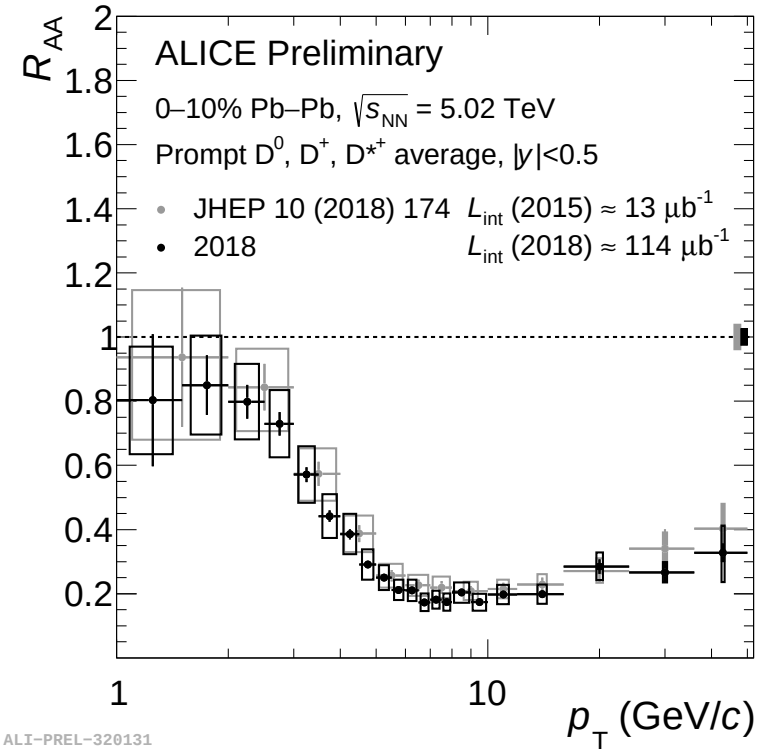

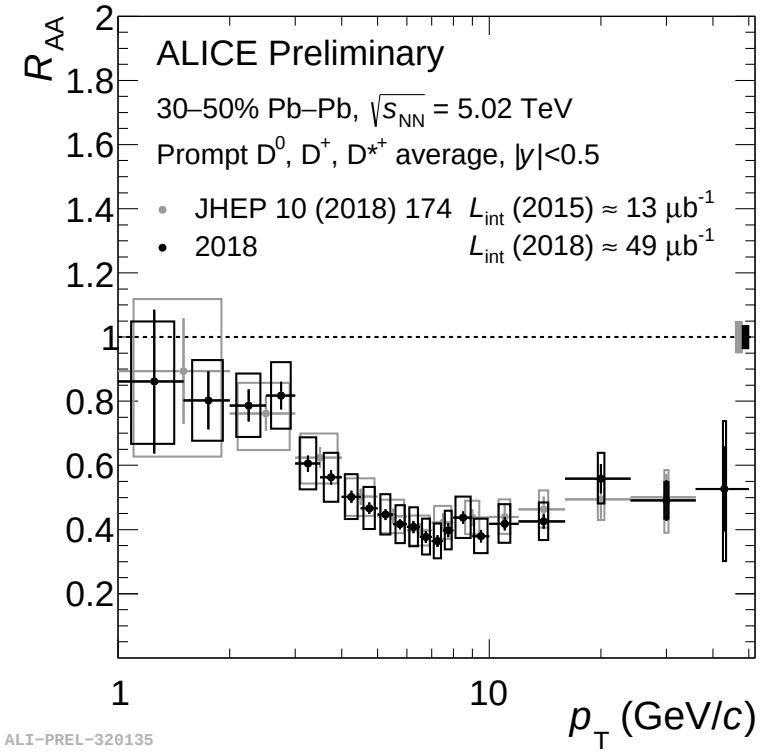

- The two measurements are compatible within their uncertainties
- Higher p_{T} granularity in 2018 w.r.t. 2015

Non-strange D-meson R_{AA} in Pb-Pb collisions

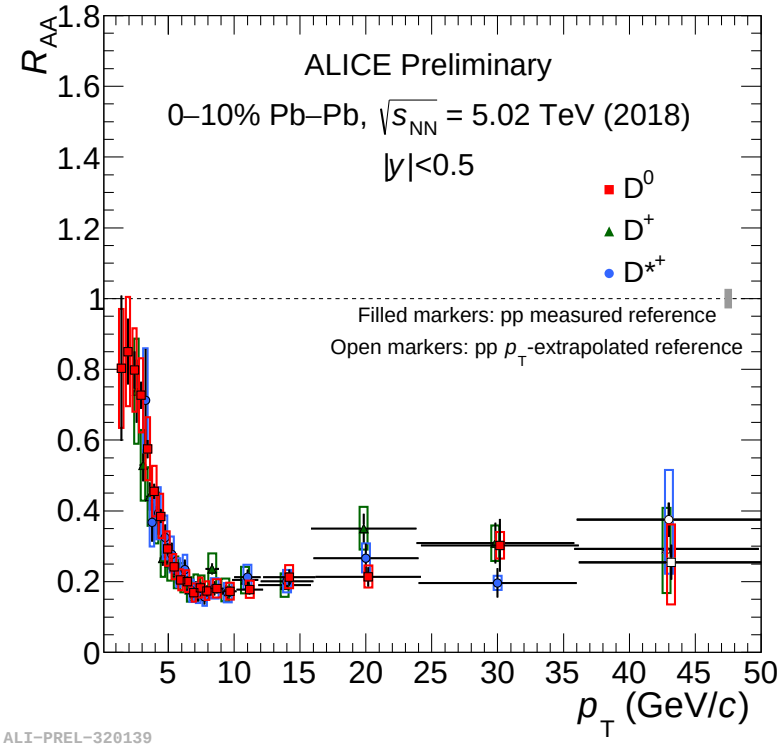

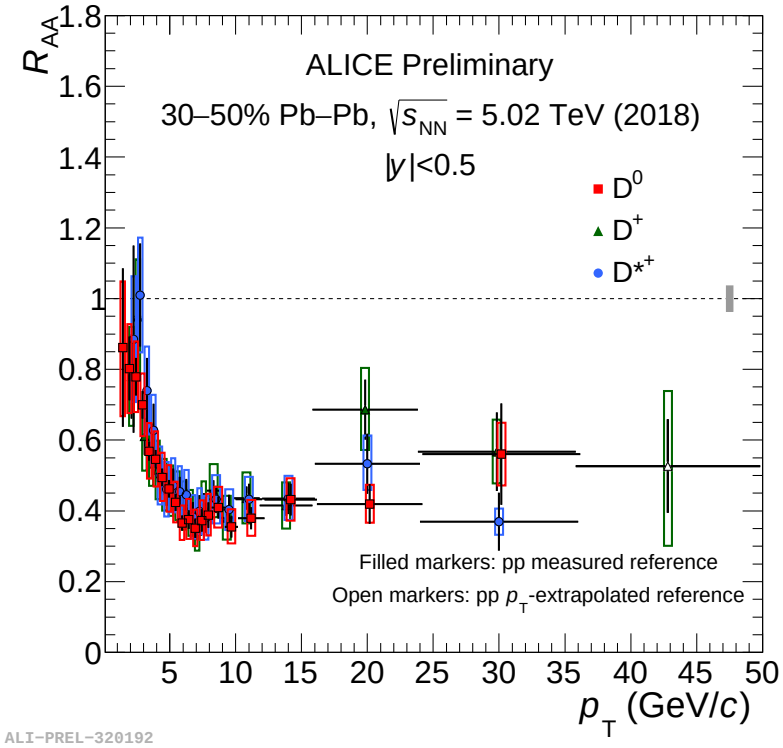

- D^0, D^+ and D^{*+} R_{AA} are compatible within their uncertainties
- Maximum of the R_{AA} suppression (factor ~ 5 and ~ 2.5) at $8 - 12$ GeV/c in $0 - 10\%$ and $30 - 50\%$ centrality classes

Non-strange D-meson R_{AA} — Model comparison

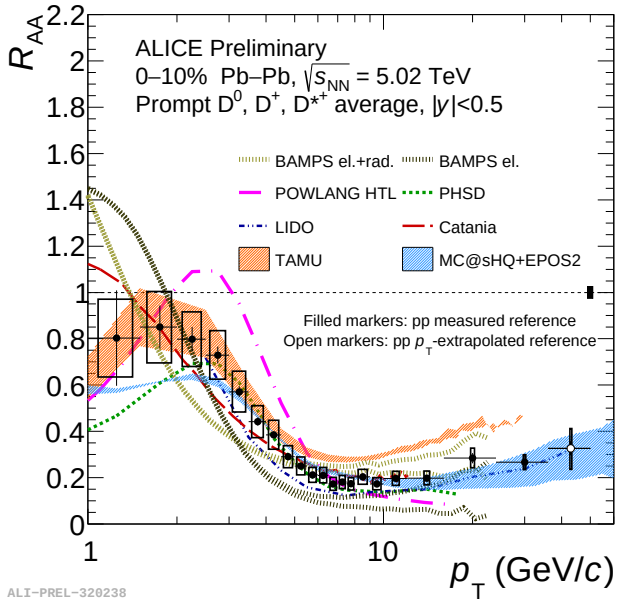

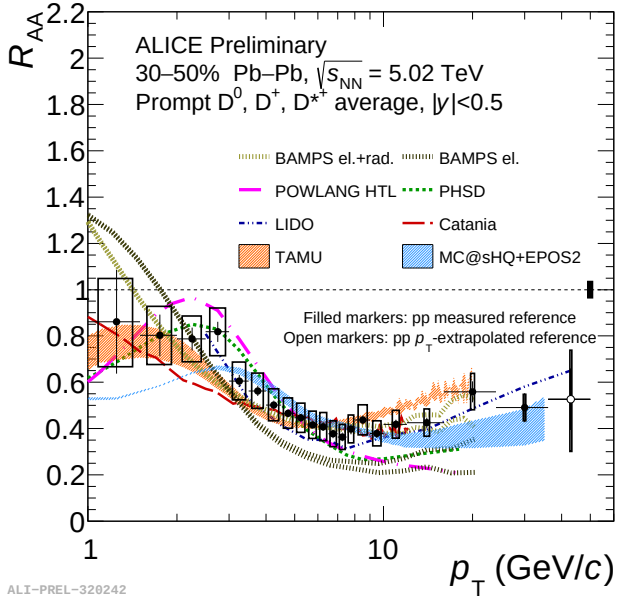

- Transport models based on Boltzmann/Fokker-Plank/Langevin equations

Transport Models	Collisional en. loss	Radiative en. loss	Coalescence	Hydro	nPDF
BAMPS	✓	✓	✗	✓	✗
POWLANG	✓	✗	✓	✓	✓
PHSD	✓	✗	✓	✓	✓
LIDO	✓	✓	✓	✓	✓
TAMU	✓	✗	✓	✓	✓

Non-strange D-meson R_{AA} — Model comparison

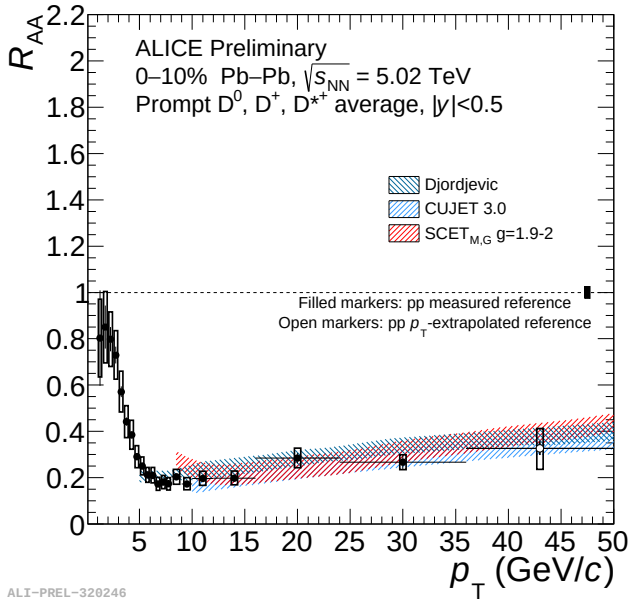

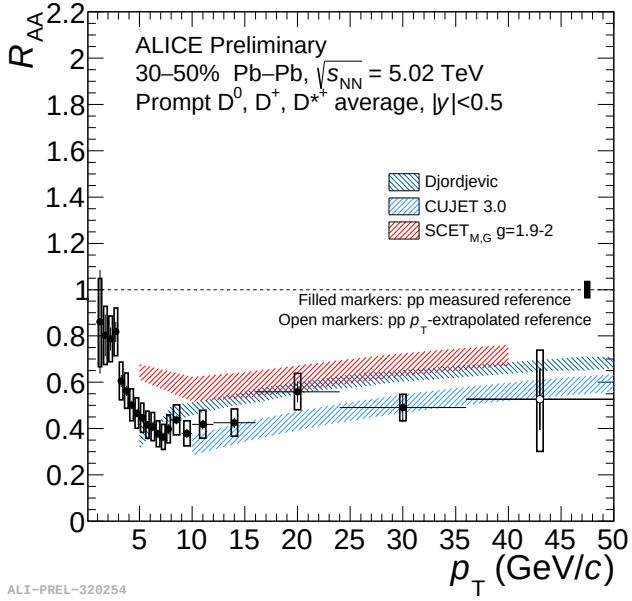

- High p_T D-meson R_{AA} described by pQCD-based models

pQCD e-loss Models	Collisional en. loss	Radiative en. loss	Coalescence	Hydro	nPDF
Djordjevic	✓	✓	✗	✗	✓
CUJET3.0	✓	✓	✗	✗	✗
SCET	✓	✓	✗	✗	✓
MC@sHQ+EPOS	✓	✓	✓	✓	✓

D-meson elliptic flow in Pb-Pb collisions

- D-meson v_2 measured at mid-rapidity ($|y| < 0.8$) with the scalar-product (SP) method

$$v_2\{SP\} = \frac{\langle \boldsymbol{u}_2 \cdot \boldsymbol{Q}_2^{\mathrm{A}} / M^{\mathrm{A}} \rangle}{\sqrt{\frac{\langle \boldsymbol{Q}_2^{\mathrm{A}}/M^{\mathrm{A}} \cdot \boldsymbol{Q}_2^{\mathrm{B}}/M^{\mathrm{B}} \rangle \langle \boldsymbol{Q}_2^{\mathrm{A}}/M^{\mathrm{A}} \cdot \boldsymbol{Q}_2^{\mathrm{C}}/M^{\mathrm{C}} \rangle}{\langle \boldsymbol{Q}_2^{\mathrm{B}}/M^{\mathrm{B}} \cdot \boldsymbol{Q}_2^{\mathrm{C}}/M^{\mathrm{C}} \rangle}}}$$

where $\boldsymbol{Q}_2 = \sum_{j=0}^{M} w_j e^{i2\varphi_j}$ and $\boldsymbol{u}_{2,D} = e^{i2\varphi_D}$

- Sub-events:
  - A: V0C ($-3.7 < \eta < -1.7$)
  - B: V0A ($2.8 < \eta < 5.1$)
  - C: TPC ($|\eta| < 0.8$))

- v_2 of the signal extracted from a v_2 vs mass fit

$$v_2(M) = \frac{S}{S+B} v_2^{sig} + \frac{B}{S+B} v_2^{\mathrm{bkg}}$$

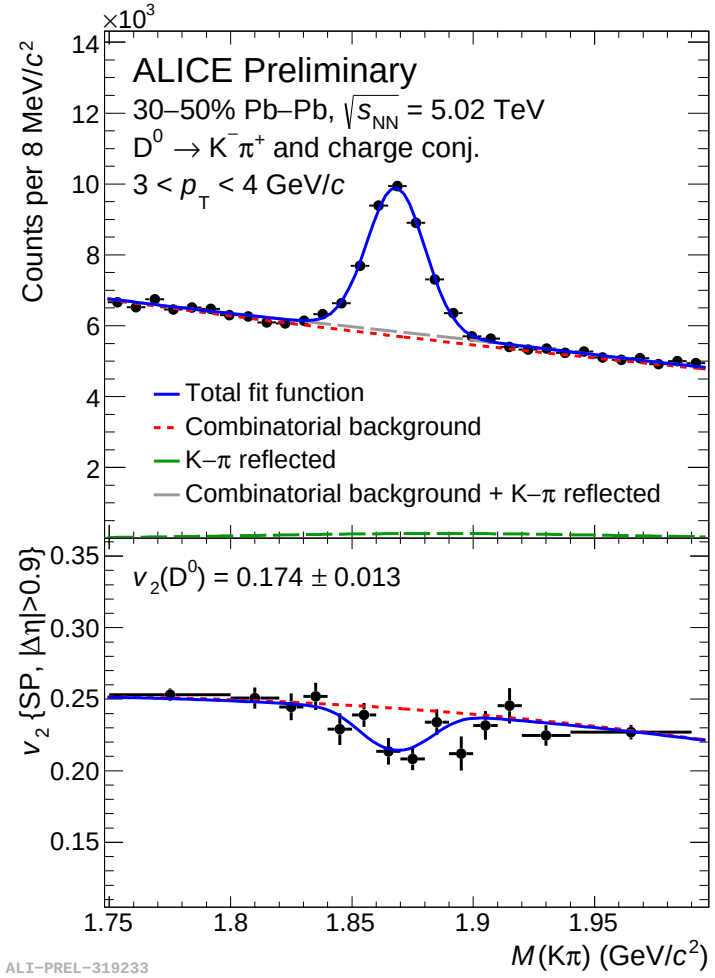

Non-strange D-meson v2 — Comparison with 2015 data

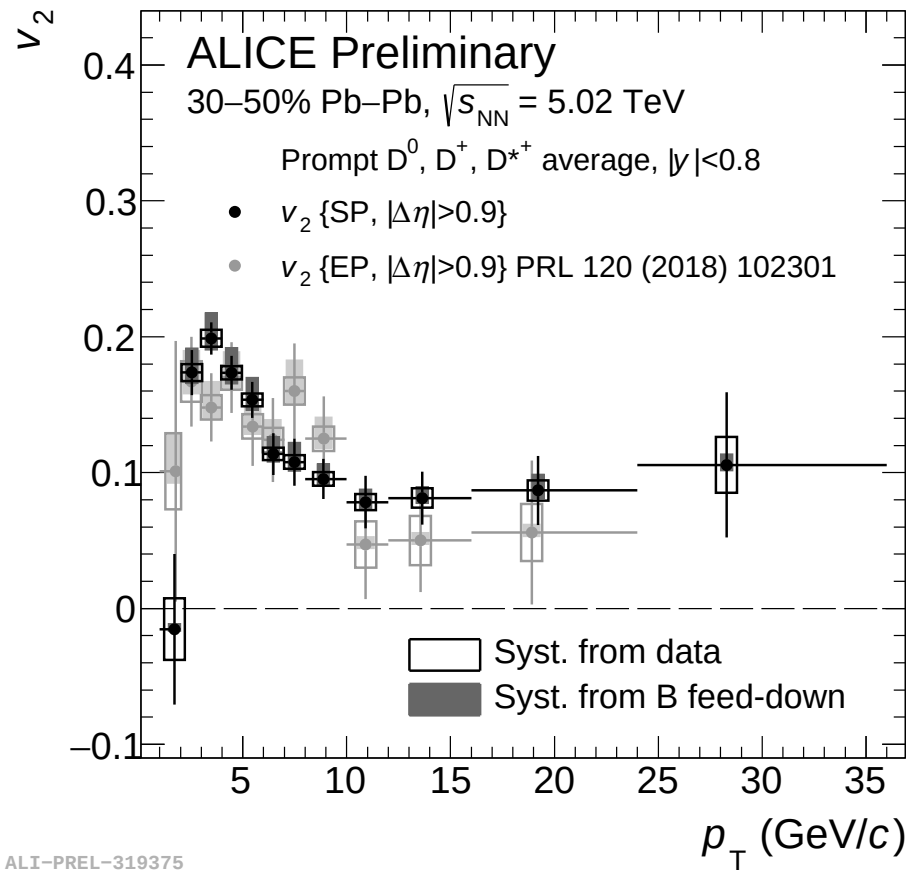

- The two measurements are compatible within their uncertainties
- Statistical uncertainty reduced by a factor ~ 2 in 2018
- Extended p_{T} coverage up to 36 GeV/c

Effect of detector resolution in ESE selection

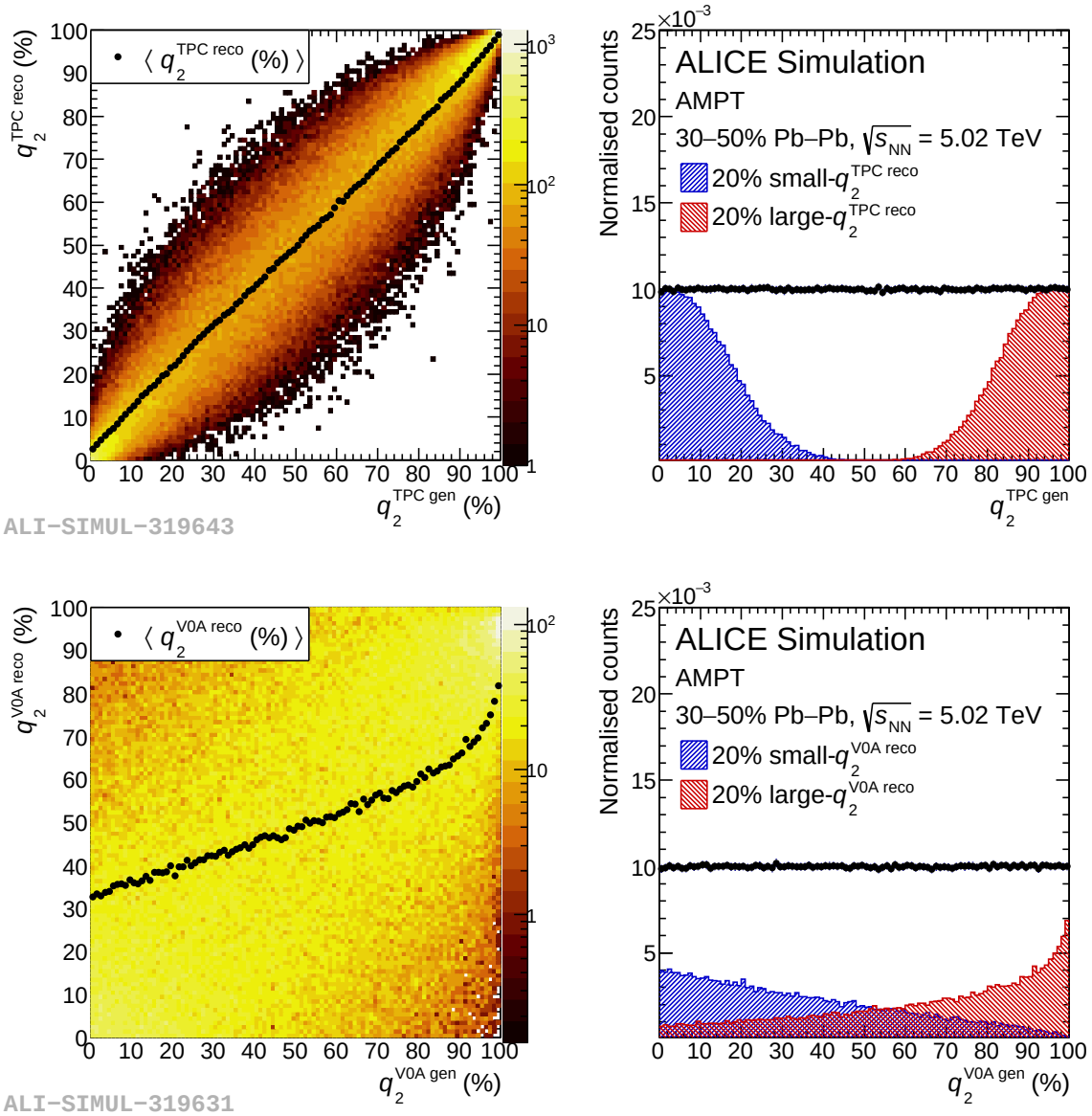

- Small effect from detector resolution in case of q_2^{TPC}, while significant smearing of q_2 distribution in case of q_2^{V0A} due to resolution in azimuthal angle

ESE for D-meson yields

POWLANG: EPJC (2019) 79: 494

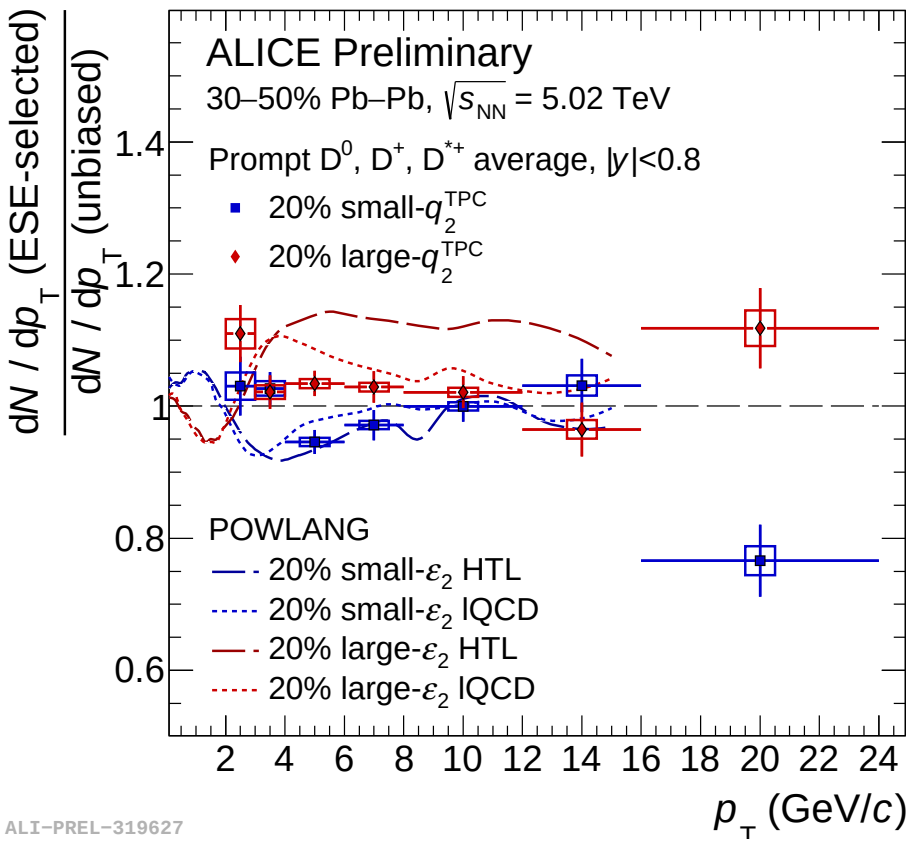

- Hint of higher (lower) p_T-differential yields in large-q_2 (small-q_2) samples compared to the unbiased one at intermediate p_T
  - consistent with correlation between radial and elliptic flow

- Measurement quantitatively in agreement with the POWLANG prediction in the small-q_2 sample, while smaller effect observed in large-q_2 sample

Further studies

Very nice preliminary results! Still room for improvements:

- Candidate selection based on machine learning techniques
  - $\mathrm{D_s^+}$ measurement at lower p_T to better constrain the models
  - reduce the R_AA statistical uncertainty for the $\mathrm{D_s^+}$ and $\mathrm{D^0}$ (at low p_T) mesons

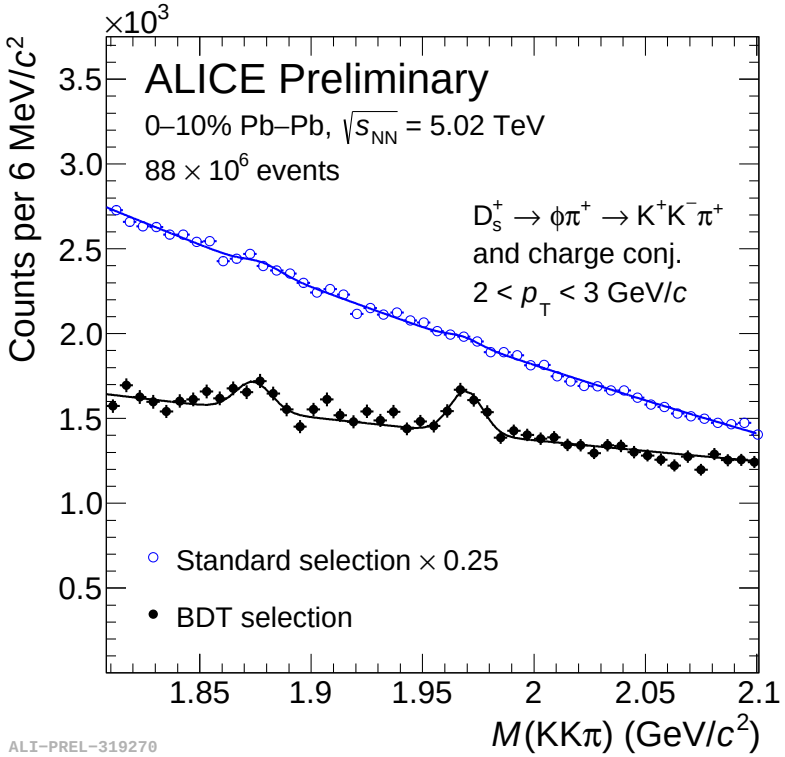

- $\mathrm{D^0}$ analysis without topological cuts ➔ to reach lower transverse momenta